J. Phys. Chem. A **1999,** *103,* 5137−5151

Structural, Rotational, Vibrational, and Electronic Properties of Ionized Carbon Clusters C_n^+ ($n = 4-19$)

M. G. Giuffreda, M. S. Deleuze,* and J.-P. François

Limburgs Universitair Centrum, Institute for Materials Science (IMO), Departement SBG, Universitaire Campus, B-3590 Diepenbeek, Belgium

Received: December 16, 1998; In Final Form: April 26, 1999

The structures, rotational moments, vibrational normal modes, and infrared spectra of small to medium-size ionized carbon clusters C_n^+ ($n = 4-19$) are investigated using density functional (DFT) and coupled cluster (CC) theories. Comparison is made with the neutral systems from which they derive. In contrast to previous restricted open-shell Hartree−Fock (ROHF) results by von Helden and co-workers, electron correlation is shown to strongly limit distortions of the structure upon an adiabatic ionization process. Nonetheless, for such a process, the C_{4n+2} and to a lesser extent the C_{4n+1} cyclic systems are found to evolve from an essentially regular (i.e., cumulenic) pattern to a more alternating (i.e., polyynic) structure in their ionized forms, whereas the opposite trend is observed for the C_{4n} and C_{4n+3} rings. Similarly, linear carbon clusters, which can be regarded as mostly cumulenic in their neutral form, tend to become more polyynic after ionization. Rotational moments, IR spectra, and adiabatic ionization potentials as well should provide specific markers of these contrasted characters and behaviors. It has been found that the linear cations show a much more pronounced IR intensity than the cyclic ones. Many of the studied species show a strong absorption in certain regions of the spectrum (e.g., around 2036 cm^{-1}).

Introduction

Carbon clusters C_n (refs 1−4 and references therein) are important species in research fields as diverse as astrophysics, material sciences, and combustion processes. C_n clusters of various sizes have, e.g., been identified in comet tails and in stellar atmospheres, and a large number of these compounds have been detected in the interstellar space.[5−8] C_n clusters are of major and direct interest in material sciences, since they play a key role in the preparation of thin diamond films via chemical vapor deposition or cold plasma techniques.[9−11] Theoretical investigations on carbon nanoclusters are also very topical, owing to their close relationships with fullerenes[11−14] and their importance in the formation of carbon cages.[15] A comprehensive understanding of their structure and energetics is at last required for a better catalytic control of their formation and combustion.[16]

The structures and vibrational spectra of neutral C_n clusters have been already characterized thoroughly, either theoretically or experimentally (refs 1−6 and 16−19 and references therein). On the other hand, the structural and spectroscopic properties of ionized C_n^+ species have not been investigated in detail yet. Traditional spectroscopic methods can only be applied with great difficulty to ionized and highly reactive nanoclusters, and experimentalists rely heavily on theoretical data to safely interpret measurements on such exquisitely exotic systems. Only one series of experimental investigations, based on gas-phase ion chromatography,[20,21] has been reported for C_n^+ clusters with $n = 7-10$. These have been analyzed[22] on the grounds of calculations at the ROHF (spin-restricted open-shell Hartree−Fock) level, a rather questionable approximation in view of the importance of electron correlation within such systems. These studies show that carbon cluster cations have cyclic and linear isomers, which for the heavier C_n^+ species coexist with significant percentages in the samples under investigation. Either for the linear or the cyclic forms of C_n^+ species, ROHF calculations yield a pronounced polyynic-like[23] pattern of single and triple bond alternation, with bond lengths oscillating typically between 1.19 and 1.38 Å.[22] However, the main concern with calculations at the HF level arises precisely from the instability of the wave function of strongly correlated systems toward geometrical distortions. This yields in general a strong overestimation of the alternating character of chains with a small electron band gap, a limiting case being the Peierls distortion of infinitely large metallic chains.[24]

Another important aspect of carbon clusters is their vibrational structure, which, through the interplay of selection rules,[25] provides a direct experimental information on the nature of the chemical bonds and groups. However, although it is possible to produce ionic species as well as neutral carbon clusters, there are very few experimental spectroscopic and structural studies reported for carbon cluster cations with $n \geq 5$. In general, the recorded spectra are difficult to interpret safely, as the investigated plasmas are most often complex mixtures of several species comprising neutral, cationic, but also possibly anionic clusters in the usual conditions. One example is a Fourier transform IR (FTIR) study of the cyclic C_5^+ cluster produced by laser vaporization of graphite and trapped in a solid argon matrix at 12 K.[26] Accurate theoretical data are therefore highly necessary.

In the present paper, taking advantage of the tremendous advances realized over the past few years in computer performances, we report an exhaustive study of the structural, rotational, and vibrational properties of carbon cluster cations C_n^+ ranging from $n = 4$ to 19, using density functional theory (DFT)[27] and the highly demanding CCSD(T) treatment (coupled cluster ansatz, including single and double excitations and a perturbative estimate of triple excitations), a benchmark for most

---

* To whom correspondence should be addressed.

10.1021/jp984757c CCC: $18.00

quantum chemical studies.[28−30] Harmonic frequencies and infrared (IR) absorption activities, as well as the vibrational zero-point energy, are also evaluated using DFT. As will be shown in the present contribution, studies of the ionization properties and of the geometrical deformations induced by ionization are also quite instrumental to provide a consistent classification of the electronic and structural properties of these very peculiar systems.

Methods

In a comprehensive and systematic study of molecular chains or rings of increasing size, the first problem that arises is the selection of a sufficiently accurate but still tractable method. Ideally, any theoretical investigation of highly reactive clusters should cope with the very strong nondynamical (static) correlation effects present in their ground states. One should consider, among others, calculations at the CASPT2 (complete active space with second-order perturbation theory)[31] or CCSD(T) levels of theory. Except for clusters of relatively modest size, the tremendous cost of such methods, especially CCSD(T), still prevents a full optimization of their molecular structures. Thus, one has to compromise over accuracy if investigations on large systems are to be attempted and/or if relationships with the worlds of polymers or fullerenes are to be established. Since the most reliable post-HF methods are essentially untractable on large compounds, the first treatment that comes to mind in this context is density functional theory (DFT).[27] As already reported in several instances (see, e.g., ref 32), and as it will be shown again, DFT techniques (in conjunction with an appropriate basis set) can provide structural and vibrational results of a quality comparable to that of CCSD(T) calculations.

In the present contribution, DFT calculations have been performed using the Becke three-parameter Lee−Yang−Parr (B3LYP)[33,34] and the Becke three-parameter Perdew−Wang-91 (B3PW91)[33,35] functionals. Geometries and vibrational frequencies have been obtained at the B3LYP and B3PW91 levels in conjunction with a correlation-consistent polarized valence double-ζ (cc-pVDZ) basis set for carbon which is a [3s2p1d] contraction of a (9s4p1d) primitive set.[36]

The DFT calculations have been carried out using the GAUSSIAN 94 package[37] running on two IBM RS/6000 model 365 workstations at Limburgs Universitair Centrum. For the CCSD(T) calculations, use has been made of the MOLPRO program package.[38] Geometry optimizations of C_9^+ at the CCSD(T) level have been performed using ACES II.[39] The structure of the ionized carbon clusters have been optimized starting from the geometry of the corresponding neutral forms.[18]

Results and Discussion

1. B3LYP versus B3PW91 and CCSD(T)/cc-pVDZ. In a previous study,[32] three important features clearly emerged from test calculations on small molecules (C_2H_4, C_6H_6, furan, ...). First, it was shown that geometries obtained at the B3LYP/cc-pVDZ level are quantitatively comparable to the results of CCSD(T)/cc-pVDZ calculations. Second, enlarging the basis set beyond cc-pVDZ does not yield any appreciable improvement. Third, the accuracy of harmonic frequencies at the B3LYP/cc-pVDZ is slightly inferior to that at the CCSD(T)/cc-pVDZ level. In a separate study[40] on the same set of molecules, it was found that geometries fully optimized at the B3PW91/cc-pVDZ level are practically identical to those obtained with B3LYP/cc-pVDZ; the harmonic frequencies at both theoretical levels are furthermore nearly the same. Hence, on the premises of these studies, it has been decided to start the present exhaustive study of the structure and vibrations of ionized carbon clusters by assessing the reliability of DFT calculations within the cc-pVDZ basis, using the B3LYP and B3PW91 functionals, against the results of a full geometry optimization of the linear C_9^+ structure at the CCSD(T) level. Both functionals provide practically the same geometries (Table 1) and harmonic frequencies (Table 2) and are found furthermore to sustain a rather satisfactory comparison with the results of a full CCSD(T) geometry optimization. In view of this overall excellent agreement and in order to limit the computational cost of these exceedingly demanding calculations, energy differences for the C_n^+ isomers have been evaluated at the CCSD(T) level from single-point calculations using the B3LYP geometries. One goal of these single-point calculations will thus be in turn to evaluate the accuracy of isomerization energies obtained with the two functionals.

TABLE 1. Optimized Geometries (Å, deg) of C_9^+at the B3LYP, B3PW91, and CCSD(T)/cc-pVDZ Levels

C_9^+	B3LYP/ cc-pVDZ		B3PW91/ cc-pVDZ		CCSD(T)/ cc-pVDZ	
C_{2v}cyclic doublet ($^2B_1$)	r_{12}	1.319	r_{12}	1.318		
	r_{32}	1.278	r_{32}	1.278		
	r_{43}	1.355	r_{43}	1.352		
	r_{54}	1.250	r_{54}	1.250		
	r_{65}	1.366	r_{65}	1.363		
	θ_{123}	117.0	θ_{123}	117.0		
	θ_{234}	159.3	θ_{234}	160.1		
	θ_{345}	126.7	θ_{345}	126.2		
	θ_{456}	144.6	θ_{456}	144.7		
	θ_{219}	164.8	θ_{219}	165.9		
$D_{\infty h}$ linear doublet	r_{12}	1.324	r_{12}	1.325	r_{12}	1.343
	r_{32}	1.285	r_{32}	1.284	r_{32}	1.301
	r_{43}	1.290	r_{43}	1.289	r_{43}	1.305
	r_{54}	1.284	r_{54}	1.283	r_{54}	1.299

TABLE 2. Harmonic Frequencies (cm^{-1}) and IR Intensities (km/mol) of C_9^+ at B3LYP and B3PW91cc-pVDZ Levels[a]

C_9^+	B3LYP/cc-pVDZ	B3PW91/cc-pVDZ
C_{2v} cyclic doublet ($^2B_1$)	34(b_2, 93), 65(a_2, *), 124(b_2, 7), 226(a_2, *), 262($b_{1,}$ 0), 283(a_1, 0), 371(a_2, *), 372(b_1, 0), 405(b_1, 1), 490(b_2, 0), 509(a_1, 0), 562(a_1, 62), 903(a_1, *), 957(b_2, 221), 1083(a_1, 0), 1136(b_2, 79), 1345(a_1,10), 1800(b_2,67), 1955(a_1, 341), 2001(b_2, 163), 2072(a_1, 82)	24(b_2, 92), 96(a_2, *), 111(b_2, 9), 224(a_2, *), 262(b_1, 0), 280(a_1, 0), 370(a_2, *), 373(b_1, 0), 409(b_1, 1), 489(b_2, 1), 508(a_1, 0), 552(a_1, 56), 912(a_1, 3), 1093(a_1, 0), 1101(b_2, 0), 1357(a_1, 9), 1816(b_2, 71), 1971(a_1, 341), 2004(b_2, 175), 2092(a_1, 88)
$D_{\infty h}$ linear doublet	44(6), 50(2), 78(0),122(*), 125(20), 207(4), 238(0), 287(*), 434(4), 461(σ_g, 0), 506(0), 601(0), 611(*), 716(10), 737(0), 876(σ_u, 78), 1258(σ_g, *), 1575(σ_u, 357), 1832(σ_u, 4187) 1897(σ_g, *), 2108(σ_u, 2133), 2187(σ_g, *)	49(2), 57(0), 120(*), 193(*), 201(4), 284 (*), 411(5), 463(σ_g,*), 508(*), 592(*), 612(*), 726(10), 743(0), 878(σ_u, 83), 1261(σ_g, *), 1581(σ_u, 403), 1854(σ_u, 4192), 1905(σ_g, *), 2117(σ_u, 2075), 2200(σ_g, *)

[a] (*) represents IR inactive frequencies and (0) indicates very small intensities (<0.6 km/mol).

2. Structural Considerations on Cyclic Clusters. All the cyclic carbon cluster cations considered in the present study have been found to be strictly (or practically) *planar* (Figure

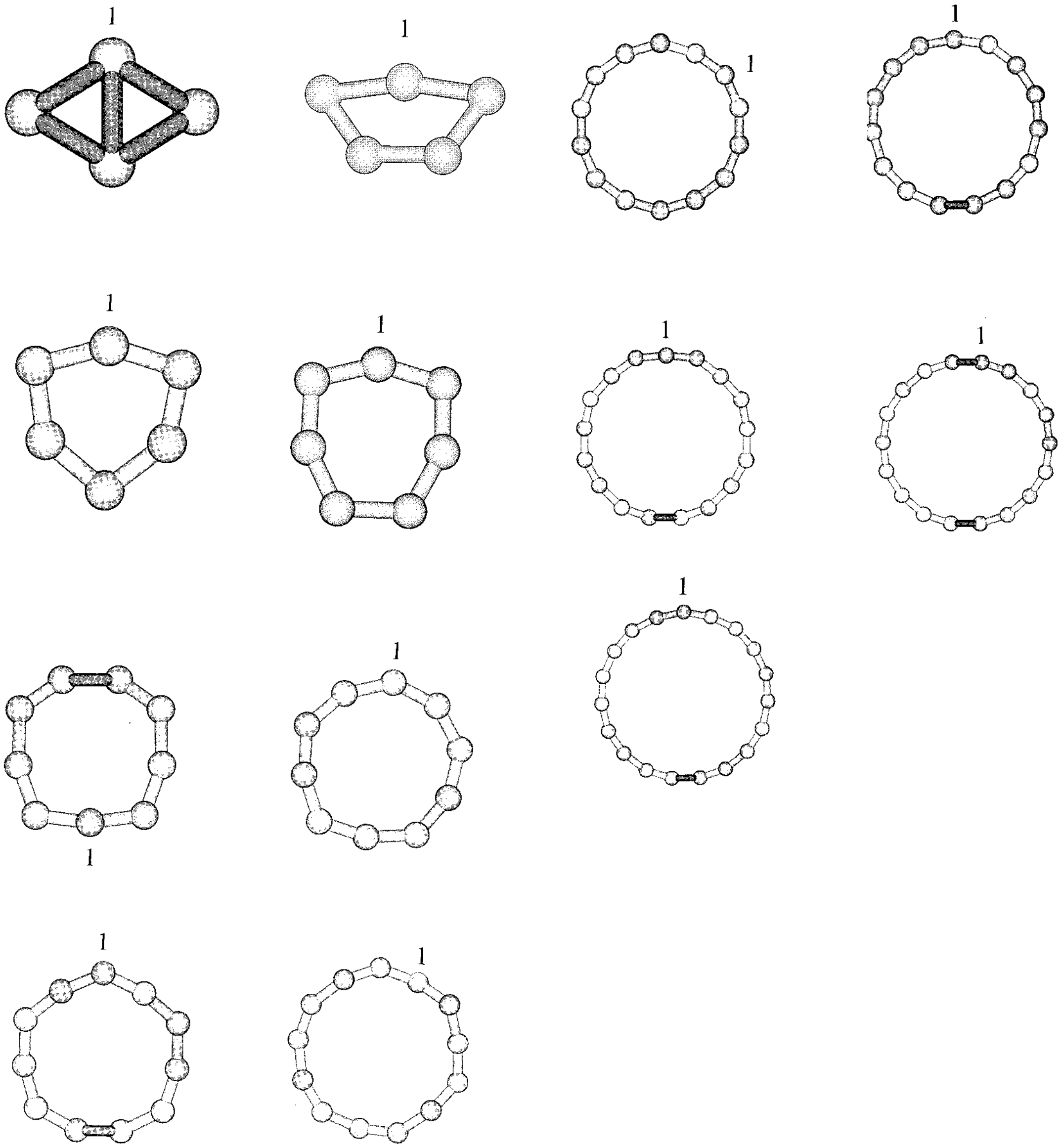

Figure 1. Structures of the investigated cyclic clusters C_n^+ ($n = 4-7, 9-11, 13-15, 17-19$). All bond lengths and bond angles are equivalent in C_8^+ (C_s), C_{12}^+ (D_{6h}), and C_{16}^+ (D_{8h}).

1). This is in particular the case for the C_5^+ and C_9^+ species, the neutral counterparts of which exhibit[18] a slight but net deviation from planarity. Releasing symmetry constraints in a B3LYP optimization of C_9^+, for instance, does not yield distortions from planarity larger than 0.014 Å (deviations measured from the average plane of the ring). The corresponding energy lowering does not exceed 8 cal/mol. The bond lengths of the cyclic C_n^+ cations in their doublet and quartet states are collected in Table 3. For completeness and comparison purposes, we have also included in that table the geometrical parameters of the corresponding neutral species in their ground singlet states. To simplify the comparison, we present in Table 4 the bond length alternations defined as the absolute values of the differences between successive bond lengths of the neutral (singlet states) and ionized (doublet states) cyclic C_n clusters.

In close parallelism with the neutral species,[18] it is found that the C_{4n}^+ species ($n = 2-4$) display a clear alternation pattern of short "C≡C" and large "C−C" bond lengths and can therefore be referred to as "*polyynic*",[23] whereas the C_{4n+2}^+ species ($n = 1-4$) are essentially nonalternating and can thus be described as "*cumulenic*",[18] in sharp contrast to the conclusions drawn by von Helden et al.[22] from their ROHF calculations on C_6^+ and C_{10}^+. ROHF theory yields a much too pronounced polyynic pattern, in the form of a strong alternation of bond lengths, as a result of an instability of the ROHF wave function toward geometrical distortions. This deficiency is clearly remedied when electron correlation is included. The chemical bonding characteristics of cyclic C_n^+ clusters, as well as of their neutral counterparts, are thus reminiscent of the Hückel topological rules for the $4n$ and $4n + 2$ π-electron system of antiaromatic and aromatic cyclic C_nH_n polyenes, respectively. In this case, one should also take into account that carbon clusters develop out-of-plane but also in-plane π-electron conjugation;[17] the latter prevents strong departures from planarity, as for cyclooctatetraene.[41]

In general, for the largest cyclic cations with a clearly defined polyynic character (e.g., C_8^+, C_{12}^+, C_{16}^+), correlation effects are found to yield a strong decrease of the bond length alternation, as a result of the mixture of the occupied and virtual spaces, characterized by a reversal of the bonding/antibonding pattern of molecular orbitals; for these systems, the bond lengths oscillate typically between 1.27 and 1.33 Å only. Correspondingly, for the ionized but also for the neutral systems and as shown from the data displayed in Tables 3 and 4, bond

TABLE 3. Geometries of the Cyclic C_n^+ Cations Compared with Those of the C_n Neutral Systems[a] at the B3LYP/cc-pVDZ Level

C_4^+	
$^2B_{1u}$ (D_{2h})	$r = 1.444$
$^4B_{3u}$ (D_{2h})	$r = 1.393$
^1A_g (D_{2h}) neutral[a]	$r = 1.454$
C_5^+	
$^2A'$ (C_s)	$r_{21} = 1.495$, $r_{32} = 1.326$, $r_{43} = 1.450$, $r_{54} = 1.326$, $r_{51} = 1.499$
$^4A_2$ (C_{2v})	$r_{21} = 1.402$, $r_{32} = 1.343$, $r_{43} = 1.352$
$^1A_1$ (C_2) neutral[a]	$r_{21} = 1.365$, $r_{32} = 1.436$, $r_{43} = 1.568$
C_6^+	
$^2A_1$ (C_{2v})	$r_{21} = 1.329$, $r_{32} = 1.297$, $r_{43} = 1.356$
$^4B_2$ (C_{2v})	$r_{21} = 1.355$, $r_{32} = 1.356$, $r_{43} = 1.357$
$^2A_1$ (C_{2v}) ROHF[b]	$r_{21} = 1.307$, $r_{32} = 1.272$, $r_{43} = 1.361$
$^1A'_1$ (D_{3h}) neutral[a]	$r = 1.332$
C_7^+	
$^2A'$ (C_s)	$r_{21} = 1.312$, $r_{32} = 1.310$, $r_{43} = 1.311$, $r_{54} = 1.390$, $r_{65} = 1.311$, $r_{76} = 1.310$, $r_{71} = 1.312$
$^4B_1$ (C_{2v})	$r_{21} = 1.357$, $r_{32} = 1.305$, $r_{43} = 1.282$, $r_{54} = 1.398$
$^2B_1$ (C_{2v}) ROHF[b]	$r_{21} = 1.301$, $r_{32} = 1.297$, $r_{43} = 1.301$, $r_{54} = 1.369$
$^1A_1$ (C_{2v}) neutral[a]	$r_{21} = 1.332$, $r_{32} = 1.352$, $r_{43} = 1.405$, $r_{54} = 1.270$
C_8^+	
$^2A''$ (C_s)	$r_{21} = 1.290$, $r_{32} = 1.352$
$^4A_1$ (C_{2v})	$r = 1.313$
$^2A''$ (C_s) ROHF[b]	$r_{21} = 1.337$, $r_{32} = 1.278$
^1A_g (C_{4h}) neutral[a]	$r_{21} = 1.267$, $r_{32} = 1.389$
C_9^+	
$^2B_1$ (C_{2v})	$r_{21} = 1.319$, $r_{32} = 1.278$, $r_{43} = 1.355$, $r_{54} = 1.250$, $r_{65} = 1.366$
$^4A_2$ (C_{2v})	$r_{21} = 1.314$, $r_{32} = 1.289$, $r_{43} = 1.344$, $r_{54} = 1.262$, $r_{65} = 1.374$
$^2A'$ (C_2) ROHF[b]	$r_{21} = 1.273$, $r_{32} = 1.328$, $r_{43} = 1.255$, $r_{54} = 1.340$, $r_{65} = 1.292$, $r_{76} = 1.300$, $r_{87} = 1.383$, $r_{98} = 1.221$, $r_{91} = 1.418$
^1A (C_1) neutral[a]	$r_{21} = 1.320$, $r_{32} = 1.311$, $r_{43} = 1.314$, $r_{54} = 1.314$, $r_{65} = 1.312$, $r_{76} = 1.321$, $r_{87} = 1.312$, $r_{98} = 1.335$, $r_{91} = 1.311$
C_{10}^+	
$^2B_2$ (C_{2v})	$r_{21} = 1.291$, $r_{32} = 1.309$, $r_{43} = 1.279$, $r_{54} = 1.309$, $r_{65} = 1.293$
$^4B_1$ (C_{2v})	$r_{21} = 1.299$, $r_{32} = 1.328$, $r_{43} = 1.279$, $r_{54} = 1.325$, $r_{65} = 1.295$
$^2A'$ (C_s)[b]	$r_{21} = 1.335$, $r_{32} = 1.242$, $r_{43} = 1.306$, $r_{54} = 1.269$, $r_{65} = 1.289$
$^1A'_1$ (D_{5h}) neutral[a]	$r = 1.301$
C_{11}^+	
$^2A_1$ (C_{2v})	$r_{21} = 1.299$, $r_{32} = 1.292$, $r_{43} = 1.310$, $r_{54} = 1.280$, $r_{65} = 1.324$, $r_{76} = 1.267$
$^4B_1$ (C_{2v})	$r_{21} = 1.320$, $r_{32} = 1.272$, $r_{43} = 1.351$, $r_{54} = 1.262$, $r_{65} = 1.346$, $r_{76} = 1.265$
$^2A''$ (C_s)[b]	$r_{21} = 1.300$, $r_{32} = 1.245$, $r_{43} = 1.342$, $r_{54} = 1.217$, $r_{65} = 1.362$
$^1A_1$ (C_{2v}) neutral[a]	$r_{21} = 1.303$, $r_{32} = 1.321$, $r_{43} = 1.286$, $r_{54} = 1.351$, $r_{65} = 1.255$, $r_{76} = 1.367$
C_{12}^+	
$^2A_{2g}$ (D_{6h})	$r_{21} = 1.275$, $r_{32} = 1.328$
$^4B_{1u}$ (D_{6h})	$r_{21} = 1.296$, $r_{32} = 1.272$
$^1?$ (C_{6h}) neutral[a]	$r_{21} = 1.255$, $r_{32} = 1.357$
C_{13}^+	
^2A (C_1)	$r_{21} = 1.306$, $r_{32} = 1.273$, $r_{43} = 1.330$, $r_{54} = 1.253$, $r_{65} = 1.347$, $r_{76} = 1.243$, $r_{87} = 1.351$, $r_{98} = 1.245$, $\mathrm{r}_{10,9} = 1.343$, $r_{11,10} = 1.258$, $r_{12,11} = 1.323$, $r_{13,12} = 1.280$, $r_{13,1} = 1.298$
$^4A_2$ (C_{2v})	$r_{21} = 1.298$, $r_{32} = 1.283$, $r_{43} = 1.314$, $r_{54} = 1.269$, $r_{65} = 1.325$, $r_{76} = 1.261$, $r_{87} = 1.330$
$^1A_1$ (C_{2v}) neutral[a]	$r_{21} = 1.301$, $r_{32} = 1.285$, $r_{43} = 1.315$, $r_{54} = 1.271$, $r_{65} = 1.325$, $r_{76} = 1.262$, $r_{87} = 1.328$
C_{14}^+	
$^2B_2$ (C_{2v})	$r_{21} = 1.287$, $r_{32} = 1.298$, $r_{43} = 1.277$, $r_{54} = 1.302$, $r_{65} = 1.277$, $r_{76} = 1.298$, $r_{87} = 1.287$
$^4B_1$ (C_{2v})	$r_{21} = 1.289$, $r_{32} = 1.306$, $r_{43} = 1.276$, $r_{54} = 1.313$, $r_{65} = 1.276$, $r_{76} = 1.306$, $r_{87} = 1.289$
$^1?$ (D_{7h}) neutral[a]	$r = 1.291$
C_{15}^+	
$^2B_1$ (C_{2v})	$r_{21} = 1.292$, $r_{32} = 1.280$, $r_{43} = 1.305$, $r_{54} = 1.269$, $r_{65} = 1.314$, $r_{76} = 1.262$, $r_{87} = 1.320$, $r_{98} = 1.260$
$^4A_1$ (C_{2v})	$r_{21} = 1.288$, $r_{32} = 1.306$, $r_{43} = 1.276$, $r_{54} = 1.305$, $r_{65} = 1.288$, $r_{76} = 1.287$, $r_{87} = 1.307$, $r_{98} = 1.275$
$^1A_1$ (C_{2v}) neutral[a]	$r_{21} = 1.296$, $r_{32} = 1.311$, $r_{43} = 1.280$, $r_{54} = 1.326$, $r_{65} = 1.264$, $r_{76} = 1.338$, $r_{87} = 1.251$, $r_{98} = 1.343$
C_{16}^+	
$^2?$ (D_{8h})	$r_{21} = 1.291$, $r_{32} = 1.293$
$^4?$ (D_{8h})	$r_{21} = 1.288$, $r_{32} = 1.306$
$^1?$ (C_{8h}) neutral[a]	$r_{21} = 1.296$, $r_{32} = 1.311$
C_{17}^+	
$^2B_1$ (C_{2v})	$r_{21} = 1.295$, $r_{32} = 1.277$, $r_{43} = 1.313$, $r_{54} = 1.261$, $r_{65} = 1.329$, $r_{76} = 1.250$, $r_{87} = 1.340$, $r_{98} = 1.243$, $r_{10,9} = 1.344$
$^4A_2$ (C_{2v})	$r_{21} = 1.293$, $r_{32} = 1.282$, $r_{43} = 1.303$, $r_{54} = 1.273$, $r_{65} = 1.312$, $r_{76} = 1.266$, $r_{87} = 1.318$, $r_{98} = 1.262$, $r_{10,9} = 1.320$
$^1A_1$ (C_{2v}) neutral	$r_{21} = 1.295$, $r_{32} = 1.282$, $r_{43} = 1.307$, $r_{54} = 1.271$, $r_{65} = 1.317$, $r_{76} = 1.263$, $r_{87} = 1.324$, $r_{98} = 1.258$, $r_{10,9} = 1.326$
C_{18}^+	
$^2A_1$ (C_{2v})	$r_{21} = 1.300$, $r_{32} = 1.275$, $r_{43} = 1.297$, $r_{54} = 1.281$, $r_{65} = 1.290$
$^4B_2$ (C_{2v})	$r_{21} = 1.336$, $r_{32} = 1.252$, $r_{43} = 1.325$, $r_{54} = 1.270$, $r_{65} = 1.299$
$^1?$ (D_{9h}) neutral[a]	$r = 1.288$
C_{19}^+	
$^2A_2$ (C_{2v})	$r_{21} = 1.285$, $r_{32} = 1.295$, $r_{43} = 1.276$, $r_{54} = 1.304$, $r_{65} = 1.268$, $r_{76} = 1.311$, $r_{87} = 1.263$, $r_{98} = 1.315$, $\mathrm{r}_{10,9} = 1.260$, $r_{11,10} = 1.317$
$^1A_1$ (C_{2v}) neutral	$r_{21} = 1.286$, $r_{32} = 1.301$, $r_{43} = 1.272$, $r_{54} = 1.314$, $r_{65} = 1.261$, $r_{76} = 1.325$, $r_{87} = 1.254$, $r_{98} = 1.332$, $\mathrm{r}_{10,9} = 1.250$, $r_{11,10} = 1.335$

[a] Martin, J. M. L.; El-Yazal, J.; François, J. P. *Chem. Phys. Lett.* **1995**, *242*, 570; *Chem. Phys. Lett.* **1996**, *252*, 9. [b] von Helden, G.; Gotts, N. G.; Palke, W. E.; Bowers, M. T. *Int. J. Mass Spectrom. Ion Processes* **1994**, *138*, 33. Symmetrically redundant data are not given, atoms are labelled consecutively (clockwise) according to the definitions of Figure 1, and bond lengths are in Å. For comparison purposes, the ROHF/6-31g(d) results by von Helden et al. are also included. (?) indicates that no consistent treatment of symmetry groups containing rotation axis of large but finite orders such as C_{6h}, D_{7h}, D_{8h}, D_{9h} were possible[a] with the GAUSSIAN94 package.

TABLE 4. Successive Bond Length Alternations (in Å) in Cyclic Carbon Clusters in Their Doublet States

C_4^+	0.000								
C_4	0.000								
"4*n*" Species: Polyynic									
C_8^+	0.062								
C_8	0.123								
C_{12}^+	0.052								
C_{12}	0.102								
C_{16}^+	0.002								
C_{16}	0.014								
"4*n* + 2" Species: Cumulenic									
C_6^+	0.032	0.059	0.000						
C_6	0.000	0.000	0.000						
C_{10}^+	0.018	0.030	0.029	0.016					
C_{10}	0.000	0.000	0.000	0.000					
C_{14}^+	0.011	0.021	0.025						
C_{14}	0.000	0.000	0.000						
C_{18}^+	0.025	0.022	0.016	0.009					
C_{18}	0.000	0.000	0.000	0.000					
"4*n* + 1" Species: Cumulenic									
C_5^+	0.168	0.045	0.049	0.174	0.002				
C_5	0.071	0.132	0.132	0.071	0.000				
C_9^+	0.041	0.077	0.105	0.117	0.117	0.105	0.077	0.041	
C_9	0.008	0.008	0.024	0.038	0.009	0.010	0.003	0.002	
C_{13}^+	0.033	0.057	0.077	0.093	0.104	0.104			
C_{13}	0.016	0.030	0.044	0.053	0.062	0.065			
C_{17}^+	0.018	0.036	0.052	0.068	0.080	0.091	0.097	0.101	
C_{17}	0.012	0.025	0.036	0.046	0.054	0.061	0.066	0.068	
"4*n* + 3" Species: Polyynic									
C_7^+	0.0001	0.002	0.001	0.079	0.079	0.001	0.002		
C_7	0.020	0.053	0.135	0.135	0.053	0.020	0.000		
C_{11}^+	0.008	0.018	0.030	0.044	0.057				
C_{11}	0.018	0.036	0.065	0.096	0.011				
C_{15}^+	0.013	0.025	0.036	0.045	0.052	0.058	0.060		
C_{15}	0.015	0.031	0.046	0.062	0.074	0.088	0.093		
C_{19}^+	0.010	0.019	0.028	0.035	0.043	0.048	0.053	0.055	0.057
C_{19}	0.015	0.028	0.042	0.053	0.064	0.071	0.078	0.082	0.085

alternations tend overall to diminish with increasing system size, an observation that can be related to the closure of the electronic band gap and the construction of the electron band structure[42] of a stereoregular polymer chain with metallic properties.

From a comparison with the geometrical structures of the neutral species optimized by Martin et al.[18] (see Tables 3 and 4), ionization appears to yield a significant decrease of the bond length alternation of the polyynic C_{4n} cyclic clusters, and on the contrary a slight but significant departure from a completely nonalternating pattern in the cumulenic C_{4n+2} systems. In both cases, this behavior can be easily rationalized from the topologies and degeneracies of the outermost orbitals.

In a polyynic case, e.g., C_8 (Figure 2), the two highest occupied molecular orbitals (HOMO and HOMO-1) are not degenerate and reflect the double antiaromaticity of the cluster. The HOMO ($2b_u$ in the case of C_8) is of π-symmetry and relates to the out-of-plane conjugation, whereas the HOMO-1 (e.g., the $6b_g$ level of C_8) is of σ-symmetry and arises from the in-plane conjugation. In both cases, the leading bonding overlaps can be associated to the shortest C≡C bonds. In addition, the HOMO is clearly of antibonding character in the regions corresponding to the largest C−C bonds. From inspection of the results obtained for C_8 and its cation, C_8^+, it appears that the ionized level is the HOMO-1. Furthermore, the HOMO undergoes very strong relaxation effects upon the ionization process, since it clearly ends up in a nonbonding pattern in the ionized cluster. Thus, ionization yields a net decrease of the bonding character of the shortest C≡C bonds as well as a decrease of the antibonding character associated with the largest C−C bonds, which explains the evolution of the structure toward a more regular form.

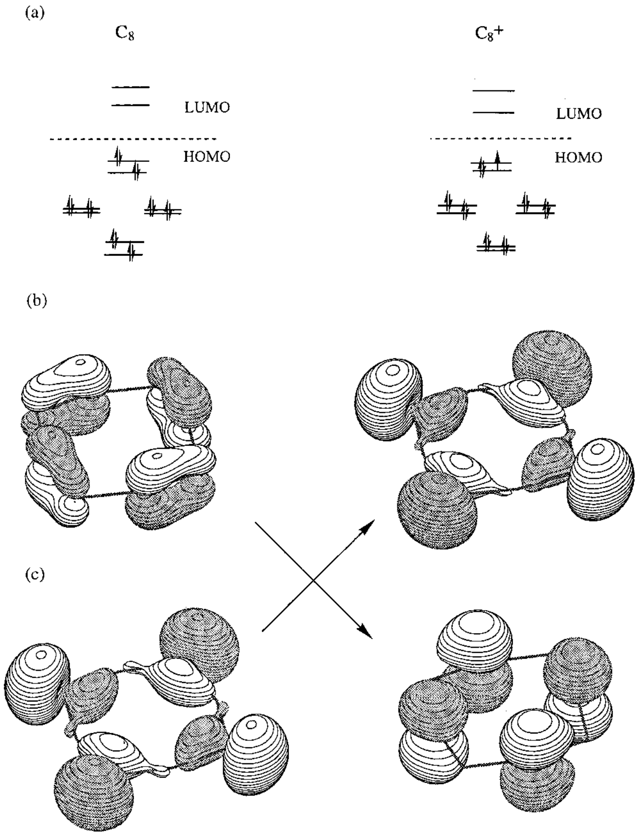

Figure 2. (a) Energy diagram for the eight outermost occupied orbitals accounting for the in-plane and out-of-plane π-electron conjugations of the C_8 and C_8^+ cyclic clusters. Schematic drawings of (b) the highest occupied molecular orbital (HOMO) and (c) the HOMO-1 orbital of these clusters.

On the other hand, the outermost electrons of cumulenic rings (e.g., C_6, Figure 3) fall in a doubly degenerate set of out-of-plane π-orbitals, which provides a fully symmetric and regular electronic distribution. Ionization of one of the frontier orbitals yields thus some asymmetrization of the electron density and hence, a distortion of the structure toward a more alternating pattern. Therefore, in this case, the distortions of cumulenic structures due to ionization can be regarded as the outcome of a Jahn−Teller effect,[43] in order to release electronic degeneracies.

Interestingly, similar trends hold also, but to a lesser extent, for the cyclic C_{4n+1} and C_{4n+3} species, which, from their ionization behavior, appear to follow the trends observed for the cumulenic C_{4n+2} and polyynic C_{4n} rings, respectively. Starting from an essentially nonalternating situation for the C_{4n+1} rings, ionization can be overall shown to yield a slight, but significant, increase of the bond length alternations, whereas for the C_{4n+3} rings, rather strongly alternating structures in the neutral state are found to become more regular in their ionized form. At this stage, it should be remarked that Hutter et al.,[2] from their DFT calculations using the local spin density exchange-correlation functional of Vosko, Wilk and Nusair[44] combined with the gradient functional of the Becke−Perdew model[45,46] and a triple-ζ basis augmented with a d-type polarization function,[47] simply reported that neutral carbon clusters with an odd-number of atoms have a ring polyynic structure with clearly alternating bond lengths. As emphasized by Hutter et al.,[2] it is quite likely that the local spin density exchange approximation represents a too limited functional for a consistent description of strongly correlated systems.

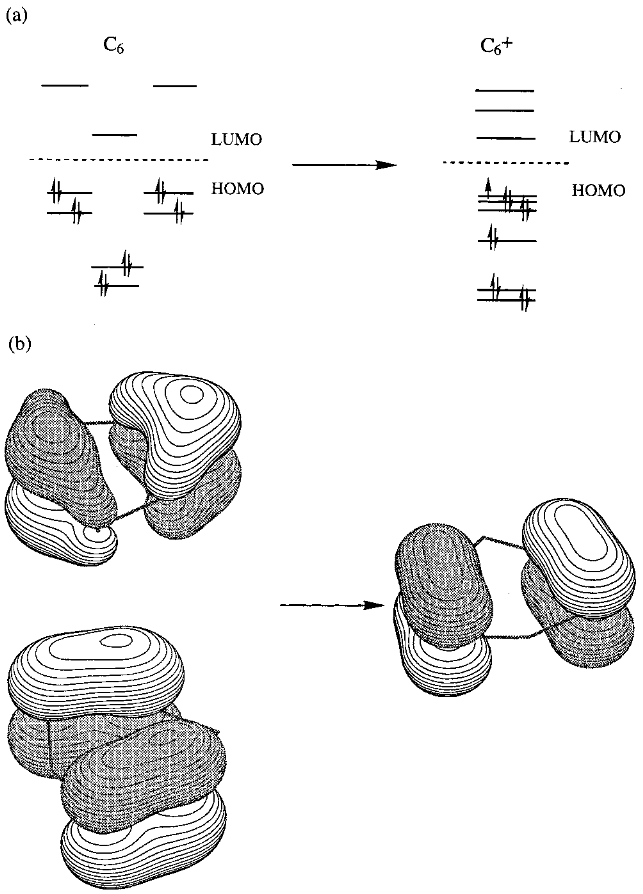

Figure 3. (a) Energy diagram for the six outermost occupied orbitals accounting for the in-plane and out-of-plane π-electron conjugations of the C_6 and C_6^+ cyclic clusters. (b) Schematic drawings of the highest occupied molecular orbitals (HOMO) and the HOMO-1 orbital of these clusters.

TABLE 5. Total Lengths (Obtained as a Sum of the Bond Lengths, in Å) and Moments of Inertia (kg m^2) of Cyclic Carbon Clusters in Their Neutral and Ionized Forms

		moments of inertia		
species	total length	I_{xx} ($\times 10^{-46}$)	I_{yy} ($\times 10^{-46}$)	I_{zz} ($\times 10^{-46}$)
Cations with an Even Number of Atoms				
C_4	5.818	2.266	6.164	8.430
C_4^+	5.769	2.855	5.449	8.304
Polyynic Structures				
C_8	10.624	22.826	22.826	45.652
C_8^+	10.567	22.545	22.550	45.095
C_{12}	15.673	74.055	74.055	148.110
C_{12}^+	15.617	73.467	73.474	146.942
C_{16}	20.764	175.097	175.097	350.194
C_{16}^+	20.669	173.802	173.802	347.604
Cumulenic Structures				
C_6	7.991	10.163	10.163	20.357
C_6^+	7.962	9.604	10.970	20.574
C_{10}	13.011	42.959	42.959	85.917
C_{10}^+	12.962	42.708	44.226	86.935
C_{14}	18.077	116.374	116.374	232.748
C_{14}^+	18.050	115.153	118.501	233.655
C_{18}	23.180	246.157	246.157	492.212
C_{18}^+	23.172	242.622	249.590	492.314
Cations with an Odd Number of Atoms				
"Polyynic" Structures				
C_7	9.447	12.670	19.068	31.738
C_7^+	9.255	14.975	16.641	31.616
C_{11}	13.031	56.102	58.179	114.281
C_{11}^+	14.275	56.636	57.853	114.488
C_{15}	19.475	141.430	144.294	285.724
C_{15}^+	19.343	143.472	144.726	287.197
"Cumulenic" Structures				
C_5	7.169	4.938	9.262	12.684
C_5^+	7.098	3.298	10.837	14.135
C_9	11.849	31.549	31.987	63.090
C_9^+	11.770	32.010	32.179	64.189
C_{13}	16.846	93.597	94.301	187.899
C_{13}^+	16.849	93.807	94.391	188.199

[a] The moments of inertia of the structures optimized at the B3LYP/cc-pVDZ level. Atomic units have been converted into SI units, using $[L] = a_0 = 5.2917 \times 10^{-11}$ m and $[M] = \text{amu} = 1.6605 \times 10^{-27}$ kg.

Since one of the most obvious tools for tracing these contrasted structural variations would be rotational spectroscopy,[48] it seemed interesting to pursue these comparisons for the moments of inertia obtained from diagonalization of the inertia tensor, i.e., $I_{qq} = \sum_J m_J q_J^2$ with $q = x, y, z$. By definition, these represent very sensitive markers of even the weakest alterations of the molecular structure. Here again, rather clear and contrasted behaviors emerge (under the influence of ionization) in particular for the systems with an even number of atoms, depending whether the C_n rings are prominently of polyynic or cumulenic character. From inspection of the results displayed in Table 5, the cumulenic C_{4n+2} clusters are found to be oblate symmetric rotors[49] in their neutral form and to become clearly asymmetric tops upon adiabatic ionization. As before, the same trend holds to a lesser extent for the cumulenic C_{4n+1} rings, as in this case ionization is also found to clearly increase the asymmetry of the rotor. In both cases, one may also note a slight but net increase of the main axis component, I_{zz}. For the polyynic C_{4n} clusters, on the other hand, the rotor remains practically symmetric, despite the lowering of the symmetry point group upon ionization (Table 3). For these species, the only detectable variations are slight decreases of the moments of inertia, which relate to a shrink of the average radius of the ring by about 0.01 Å. The trends are not so clear for the polyynic C_{4n+3} clusters. Nonetheless and interestingly, these tend to exhibit a more symmetric rotor in their ionized form.

3. Structure Considerations on Linear Clusters. The optimized structures of the linear carbon clusters considered in the present study are described, either in their neutral form (singlet states for uneven C_n species and triplets for the even ones) or in their doublet and quadruplet ionized states, in terms of the symmetry nonequivalent bond length parameters given in Table 6. As for the cyclic clusters and in order to simplify the comparison between these structures, the cumulenic or polyynic character of the chains has been evaluated from the alternations of bond lengths (Table 7). Despite end chain effects, which enforce some geometrical distortions, the structure of the C_n clusters in their neutral form can be regarded as essentially cumulenic. Furthermore, the bond length alternations tend to disappear rather quickly with the size of chains, an observation which, on the grounds of basic polymer quantum chemistry,[42] seems to indicate that infinitely large linear carbon chains would display metallic-like properties. For the smallest clusters, significant geometrical distortions toward structures with a more pronounced polyynic character can be observed in the ionized clusters. Rather unsurprisingly, the amplitude of these distortions decreases rapidly with the size of chains as well, an observation which reflects again the metallic character of the largest linear chains and their ability to delocalize charge carriers.

From the point of view of the moments of inertia (Table 8), the linear carbon clusters exhibit rather different behaviors depending on whether they are even- or odd-membered. For the C_n clusters with an even number of carbon atoms, ionization is always found to yield a slight increase of the total length of

TABLE 6. Geometries for Linear Carbon Cluster Cations at the B3LYP/cc-pVDZ Level (Bond Lengths in Å) with the ROHF/6-31G(d) Results by Von Helden et al.[b] Included for Comparison Purposes

C_4^+	
$^2?$ ($D_{\infty h}$)	1.376, 1.268
$^4\Sigma_g^-$ ($D_{\infty h}$)	1.306, 1.299
$^3\Sigma_g^-$ ($D_{\infty h}$) neutral[a]	1.319, 1.299
C_5^+	
$^2\Sigma^+$ ($C_{\infty v}$)	1.236, 1.329, 1.261, 1.336
$^4?$ ($D_{\infty h}$)	1.253, 1.303
$^1\Sigma_g^+$ ($D_{\infty h}$) neutral[a]	1.296, 1.291
C_6^+	
$^2?$ ($D_{\infty h}$)	1.347, 1.268, 1.315
$^4\Sigma^-$ ($C_{\infty v}$)	1.257, 1.306, 1.285, 1.286, 1.336
$^2\Pi$ ($D_{\infty h}$) ROHF[b]	1.327, 1.236, 1.321
$^4\Sigma^-$ ($D_{\infty h}$) ROHF[b]	1.353, 1.212, 1.372, 1.223, 1.313
$^3\Sigma_g^-$ ($D_{\infty h}$) neutral[a]	1.309, 1.296, 1.283
C_7^+	
$^2\Sigma^-$ ($C_{\infty v}$)	1.326, 1.270, 1.311, 1.251, 1.334, 1.234
$^4?$ ($D_{\infty h}$)	1.244, 1.318, 1.277
$^2\Sigma^+$ ($C_{\infty v}$) ROHF[b]	1.313, 1.233, 1.329, 1.207, 1.361, 1.191
$^1\Sigma_g^+$ ($D_{\infty h}$) neutral[a]	1.296, 1.295, 1.281
C_8^+	
$^2?$ ($D_{\infty h}$)	1.334, 1.273, 1.309, 1.263
$^4\Sigma_g^+$ ($D_{\infty h}$)	1.280, 1.230, 1.279, 1.289
$^2\Pi$ ($D_{\infty h}$) ROHF[b]	1.313, 1.241, 1.316, 1.227
$^4\Sigma^-$ ($C_{\infty v}$) ROHF[b]	1.362, 1.206, 1.344, 1.215,1.320, 1.238, 1.307
$^3\Sigma_g^-$ ($D_{\infty h}$) neutral[a]	1.305, 1.297, 1.282, 1.289
C_9^+	
$^2?$ ($D_{\infty h}$)	1.324, 1.285, 1.290, 1.284
$^4?$ ($D_{\infty h}$)	1.344, 1.282, 1.298, 1.286
$^2\Sigma^+$ ($C_{\infty v}$) ROHF[b]	1.308, 1.237, 1.321, 1.214, 1.347, 1.200, 1.370, 1.188
$^1\Sigma_g^+$ ($D_{\infty h}$) neutral[a]	1.295, 1.298, 1.280, 1.285
C_{10}^+	
$^2?$ ($D_{\infty h}$)	1.326, 1.276, 1.304, 1.264, 1.308
$^4?$ ($C_{\infty v}$)	1.322, 1.285, 1.290, 1.283, 1.282, 1.296, 1.267, 1.322, 1.244
$^2\Pi$ ($D_{\infty h}$) ROHF[b]	1.313, 1.241, 1.316, 1.227, 1.320
$^4\Sigma^-$ ($C_{\infty v}$) ROHF[b]	1.367, 1.202, 1.355, 1.207,1.338, 1.218, 1.315, 1.240, 1.304
$^3?$ ($D_{\infty h}$) neutral	1.300, 1.300, 1.281, 1.290, 1.282
C_{11}^+	
$^2?$ ($D_{\infty h}$)	1.319, 1.286, 1.290, 1.282, 1.286
$^4?$ ($D_{\infty h}$)	1.334, 1.283, 1.297, 1.281, 1.290
$^2\Sigma^+$ ($C_{\infty v}$) ROHF[b]	1.305, 1.240, 1.316, 1.217,1.340, 1.205, 1.359, 1.197, 1.375, 1.187
$^1\Sigma_g^+$ ($D_{\infty h}$) neutral[a]	1.299, 1.295, 1.287, 1.279, 1.283
C_{12}^+	
$^2?$ ($D_{\infty h}$)	1.321, 1.279, 1.301, 1.266, 1.306, 1.264
$^4?$ ($C_{\infty v}$)	1.328, 1.286, 1.289, 1.281, 1.286, 1.289, 1.277, 1.302, 1.262, 1.327, 1.241
$^3?$ ($D_{\infty h}$) neutral	1.298, 1.301, 1.280, 1.291, 1.282, 1.289
C_{13}^+	
$^2?$ ($D_{\infty h}$)	1.316, 1.287, 1.289, 1.281, 1.288, 1.284
$^4?$ ($D_{\infty h}$)	1.327, 1.284, 1.296, 1.279, 1.292, 1.285
$^1\Sigma_g^+$ ($D_{\infty h}$) neutral	1.272, 1.291, 1.262, 1.279, 1.268, 1.273
C_{14}^+	
$^2?$ ($D_{\infty h}$)	1.317, 1.281, 1.298, 1.268, 1.304, 1.265, 1.306
$^4?$ ($D_{\infty h}$)	1.319, 1.296, 1.278, 1.301, 1.266, 1.312, 1.261
C_{15}^+	
$^2?$ ($D_{\infty h}$)	1.313, 1.288, 1.288, 1.281, 1.288, 1.283, 1.286
$^4?$ ($D_{\infty h}$)	1.322, 1.285, 1.295, 1.278, 1.294, 1.281, 1.288

[a] Martin, J. M. L.; El-Yazal, J.; François, J.-P. *Chem. Phys. Lett.* **1995**, *242*, 570; *Chem. Phys. Lett.* **1996**, *252*, 9. [b] von Helden, G.; Gotts, N. G.; Palke, W. E.; Bowers, M. T. *Int. J. Mass Spectrom. Ion Processes* **1994**, *138*, 33. (?) indicates that no definite assignment of the electronic state was possible from the GAUSSIAN94 outputs.

TABLE 7. Successive Bond Length Alternations in Linear Carbon Clusters (in Å) with the ROHF/6-31G(d) Results by Von Helden et al.[a] Included for Comparison Purposes

	Species with an Even Number of Atoms								
C_4^+	0.108								
C_4	0.021								
C_6^+	0.079	0.047							
$C_6^{+\,a}$	0.091	0.085							
C_6	0.014	0.012							
C_8^+	0.061	0.034	0.046						
$C_8^{+\,a}$	0.072	0.075	0.089						
C_8	0.008	0.015	0.007						
C_{10}^+	0.050	0.028	0.040	0.043					
$C_{10}^{+\,a}$	0.072	0.075	0.089	0.093					
C_{10}	0.0001	0.019	0.010	0.008					
C_{12}^+	0.042	0.022	0.034	0.039	0.039				
C_{12}	0.003	0.021	0.011	0.009	0.007				
	Species with an Odd Number of Atoms								
C_5^+	0.092	0.068	0.074						
C_5	0.005	0.005	0.005						
C_7^+	0.056	0.041	0.061	0.084	0.100				
$C_7^{+\,a}$	0.080	0.096	0.122	0.154	0.170				
C_7	0.010	0.014	0.000	0.014	0.010				
C_9^+	0.039	0.005	0.006						
$C_9^{+\,a}$	0.071	0.084	0.107	0.133	0.147	0.170	0.182		
C_9	0.003	0.018	0.006						
C_{11}^+	0.034	0.004	0.008	0.005					
$C_{11}^{+\,a}$	0.065	0.076	0.099	0.123	0.135	0.154	0.162	0.178	0.188
C_{11}	0.005	0.021	0.009	0.004					
C_{13}^+	0.030	0.004	0.008	0.007	0.004				
C_{13}	0.020	0.029	0.016	0.005	0.000				
C_{15}^+	0.025	0.001	0.008	0.007	0.005	0.003			
C_{15}	0.007	0.024	0.012	0.009	0.005	0.003			

[a] von Helden, G; Gotts, N. G.; Palke, W. E.; Bowers, M. T. *Int. J. Mass Spectrom. Ion Processes* **1994**, *138*, 33.

TABLE 8. Total Lengths (in Å) and Moments of Inertia (in kg m^2) of Linear C_n^+ Cations[a]

species	total length (Å)	moments of inertia $I_{xx} = 0$ $I_{yy} = I_{zz}$ ($\times 10^{-46}$)
Cations with an Even Number of Atoms		
C_4	3.936	17.112
C_4^+	4.019	17.691
C_6	6.494	58.608
C_6^+	6.545	59.176
C_8	9.057	33.314
C_8^+	9.093	33.229
C_{10}	11.624	273.364
C_{10}^+	11.648	273.540
C_{12}	14.191	529.685
C_{12}^+	14.208	529.542
Cations with an Odd Number of Atoms		
C_5	5.174	33.314
C_5^+	5.161	33.229
C_7	7.744	92.753
C_7^+	7.725	92.604
C_9	10.315	198.245
C_9^+	10.365	199.153
C_{11}	12.886	363.990
C_{11}^+	12.925	364.057
C_{13}	15.290	658.684
C_{13}^+	15.487	673.260

[a] The moments of inertia of the structures optimized at the B3LYP/cc-pVDZ level. Atomic units have been converted into SI units using [L] = $a_0 = 5.2917 \times 10^{-11}$ m and [M] = amu = 1.6605×10^{-27} kg.

chains. In most cases, this induces in turn an increase of the moments of inertia, with the only exception of C_8 and C_{12}. Somewhat too simply, this relates to the fact that, in even-numbered chains, the central bond becomes markedly larger, pushing the two extremities of the chains further apart. On the contrary, for the smallest odd-membered clusters, i.e., C_5 and C_7, although ionization yields net distortions toward a polyynic pattern, only a tiny decrease of the moments of inertia can be noted. This is the result of the noncentrosymmetric character of these chains and of a very slight decrease of their total length.

For the largest odd-membered chains (C_9 to C_{13}), ionization induces again a net increase of the length of chains and correspondingly of their moments of inertia, this time as the outcome of a lowering of the bond-order of the two terminal bonds with the rest of the chain remaining essentially cumulenic.

4. Energy Considerations. The results obtained from the ion chromatography[21,50] experiments by von Helden et al.[22] provided evidence for a mixture of linear and cyclic isomers of the ionized C_n^+ ($n = 7-10$) clusters that have been generated via laser vaporization of graphite. In the same experimental conditions, the C_5^+ and C_6^+ ions were experimentally found to be purely linear, whereas the cations ranging from C_{11}^+ to C_{20}^+ appeared to be lying exclusively in their monocyclic form. As for the neutral species, this behavior arises as the natural outcome of a balance between the formation of an additional C−C bond and strains in cyclic structures based on sp-hybridized carbon atoms. These experimental findings are nicely confirmed by our calculations, since the relative energies (Table 9) show a crossing point between cyclic and linear C_n^+ species at a number of carbon atoms between 6 and 7, either with the DFT or CCSD(T) methods. At this stage, it is worth noting that the ROHF method fails in predicting the correct energy order for the C_4^+, C_7^+, and C_9^+ species, the doublet linear form being incorrectly predicted to be the most stable one (Table 9). Overall, the B3LYP, B3PW91, and CCSD(T)/cc-pVDZ theoretical levels predict the same energy sequence. One exception is C_4^+, for which the B3LYP level gives the linear doublet species as the most stable form, whereas the cyclic doublet isomer appears to be the most stable species either with the B3PW91 and CCSD(T) approaches. For C_5^+ and C_6^+, all methods predict the linear doublet as the most stable isomer. From C_7^+ to C_{19}^+, the cyclic isomers in their doublet states are clearly favored energetically.

Although they provide the same energy order, the B3LYP, B3PW91, and CCSD(T) results exhibit on the other hand some substantial variations, by several kcal/mol, in the isomerization energies. The isomerization energies obtained via the B3LYP approach deviate in average from the CCSD(T) results by 6.4 kcal/mol, whereas the B3PW91 functional yields an average deviation of 3.6 kcal/mol only. However, we found that these deviations are overall similar in magnitude to the influence on the isomerization energies of the zero-point vibrational energies and entropy effects. From preliminary investigations carried out using the RRHO (rigid rotor harmonic oscillator) approximation,[48] it seems that the latter contributions should destabilize the cyclic forms by a few kcal/mol compared to the linear forms, at ordinary temperatures.

From inspection of Table 9, the values of the so-called T_1 diagnostic[21,51] for the CCSD(T) method appear to be always larger than 0.02, reflecting the importance of nondynamical correlation and near-degeneracy effects in the ground state. It should be noted that the T_1 values are always lower than the critical value of 0.08,[52] under which the description of the ground state with a single determinant wave function is usually valid.

Compared to the results of ROHF calculations, the available DFT and CCSD(T) data obtained for the doublet states provide (Table 10) a much better agreement with the available experimental isomerization energies from the cyclic to the linear species C_n^+ (with $n = 7-10$). In regards to the fairly good agreement obtained with these experimental data, we believe that we have consistently described the structure and energetics of the C_n^+ species.

5. Vibrational Spectra. The detailed data required to simulate and/or to interpret the infrared spectra (vibrational frequencies and IR activities) of all the species considered in the present study are given in Table 11. These data have been obtained at the B3LYP level, which, as it has been shown previously, provides results comparable in quality to those of CCSD(T) calculations.

From inspection of Table 11 and an analysis of the most intense lines, it is clear that the linear carbon cations have generally a much larger IR activity than the corresponding cyclic ones. Specifically, the most intense lines of the linear cluster cations provide an IR activity between 632 and 9003 km/mol (for C_4^+ and C_{14}^+, respectively). In comparison, the most intense lines of cyclic cation clusters have an IR activity ranging typically from 100 (C_{10}^+) to 908 (C_{17}^+) km/mol only. A very weak activity, which does not exceed 21 km/mol, is found for the cyclic C_{15}^+ cluster. Overall, from the intensity of the most intense lines, the IR activity of linear cations appears from Figure 4 to grow rather regularly with the size of chains, despite a rather normal oscillation with a $2n$ periodicity. On the other hand, the size dependence of the IR activity of the cyclic species does not increase at all with the size of rings, as should be expected for a size-intensive quantity. Quite interestingly, the dotted curve displayed in Figure 4 for these species seems roughly to reflect a $4n$ periodicity, the polyynic C_{4n}^+ and cumulenic C_{4n+2}^+ cases coinciding roughly with a rise or drop of the IR activity.

From the point of view of constraints on molecular motions and the distribution of electric charges, the cyclic clusters, the smaller ones in particular, are netly disfavored. As illustrated in Figure 5, linear cations are characterized by a rather net localization of positive charges at the middle of the chain and of negative charges at the extremities (for an illustration of end-chain effects in large one-dimensional systems, see also ref 53), whereas cyclic cations naturally afford a complete delocalization of the positive charge due to ionization on the whole circumference. End chain effects in linear C_n^+ clusters thus result in particularly large and size-extensive quadrupole moments, which explains the much stronger IR activity associated with the asymmetric vibrational normal modes. Altogether, for the cyclic species, our observations suggest that polyynic, i.e., antiaromatic, structures favor a higher IR activity than cumulenic, i.e., aromatic, clusters; the smaller the band gap, the stronger the response of the system toward a perturbation, the response being in this case the change (i.e., derivative) of the dipole moment upon a distortion of the geometrical structure along the vibrational normal modes. Compared with the cumulenic, i.e., regular systems, rings of polyynic character tend to present a higher alternation of electric charges on atoms, which favors also a larger IR activity.

The smaller cyclic species (C_4^+, C_5^+) can be discriminated from the linear ones from a few intense lines with rather large intensities at low frequencies (e.g., 172, 325 cm^{-1}). When considering lines with an IR activity higher than 0.6 km/mol, it is also found that the linear species are in general marked by a larger spreading of vibrational frequencies, from 100 to 2200 cm^{-1}, than the cyclic clusters, the vibrational frequencies of which are essentially confined between 350 and 2250 cm^{-1}. This again can be related to the more strained character of cyclic structures.

In the literature, a large number of studies have been published concerning the interpretation of the IR spectrum of carbon vapor and of carbon species trapped in solid argon or krypton matrixes [refs 3, 5, 6, 18, 54, and 55 and references therein]. Vala and co-workers[26] assigned a band at 2053 cm^{-1} (Ar matrix) to cyclic C_5^+. However, Szczepanski et al.[56] proved

TABLE 9. Relative Energies (kcal/mol) of Different Structures of C_n^+ (n = 4−19) at Different Theoretical Levels (cc-pVDZ Basis Set)

	ROHF	B3LYP	B3PW91	CCSD(T)	T_1 diagnostic	CI-SD+**Q**[a,b]
C_4^+						
lin doublet	−150.794920	−151.695631	3.8	2.9	0.029	
cyc doublet	30.0	1.2	−151.622498	−151.284628	0.020	
lin quartet	54.0	6.7	7.5	8.3	0.027	
cyc quartet	4.9	13.2	4.4	15.9	0.045	
C_5^+						
lin doublet	−188.667966	−189.817357	−189.726509	−189.290094	0.036	
cyc doublet	77.9	50.1	40.9	46.8	0.027	
lin quartet	26.1	30.9	26.7	33.6	0.045	
cyc quartet	71.7	70.8	61.0	69.1	0.025	
C_6^+						
lin doublet	−226.504666	−227.908773	−227.795241	−227.262749	0.031	−227.2327
cyc doublet	19.5	11.2	0.8	2.9	0.042	4.3 ($^2A'$)
lin quartet	7.0	7.3	1.7	9.8	0.050	22.2
cyc quartet	33.7	32.7	20.8	25.8	0.036	
C_7^+						
lin doublet	−264.364470	19.6	24.0	20.9	0.032	20.5($^2\Sigma^+$)/30.0 ($^2\Pi$)
cyc doublet	3.9	−266.038734	−265.920748	−265.286077	0.043	3.2 −265.2409 ($^2B_1$)
lin quartet	27.1	49.7	49.9	52.7	0.044	
cyc quartet	69.5	65.5	61.0	65.0	0.055	
C_8^+						
lin doublet	2.2	5.1	13.2	9.1	0.032	12.0
cyc doublet	−302.203754	−304.111703	−303.977158	−303.243261	0.057	2.8 −303.1943
lin quartet	32.3	27.2	21.5	38.5	0.045	
cyc quartet	39.0	16.1	15.5	14.3	0.030	
C_9^+						
lin doublet	−340.043888	1.7	8.8	13.1	0.039	14.4($^2\Sigma^+$)/20.9 ($^2\Pi$)
cyc doublet	7.0	−342.201531	−342.048883	−341.228306	0.033	−341.1626 ($^2A''$)
lin quartet	16.2	29.8	35.6	45.8	0.052	
cyc quartet	26.7	8.1	7.6	12.0	0.034	
C_{10}^+						
lin doublet	18.8	40.7	47.9	46.5	0.033	40.5
cyc doublet	−377.918023	−380.354151	−380.184308	−379.260361	0.052	−379.1713 ($^2A'$)
lin quartet	33.8	54.2	56.3	61.1	0.048	
cyc quartet	83.4	81.5	81.3	86.4	0.030	
C_{11}^+						
lin doublet	34.2	49.8	48.5	56.2	0.040	
cyc doublet	−415.781936	−418.460453	−418.272092	−417.251382	0.048	
lin quartet	46.0	73.3	68.2	85.0	0.058	
cyc quartet	43.3	54.0	45.9	54.2	0.045	
C_{12}^+						
lin doublet	15.8	37.5	43.1	40.6	0.034	
cyc doublet	−453.596457	−456.529154	−456.322955	−455.203450	0.051	
lin quartet	31.9	52.6	52.9			
cyc quartet	14.5	8.8	7.4	7.0	0.025	
C_{13}^+						
lin doublet	36.7	36.8	43.8	47.5	0.041	
cyc doublet	−491.466154	−494.617712	−494.395673	−493.187748	0.033	
lin quartet	45.2	57.0	62.6			
cyc quartet	26.5	5.7	4.9	10.1	0.027	
C_{14}^+						
lin doublet	33.0	64.0	70.5			
cyc doublet	−529.304083	−532.747955	−532.509807	−531.197814	0.020	
lin quartet	34.2	80.1	86.3			
cyc quartet	64.0	61.5	61.8	65.4	0.018	
C_{15}^+						
lin doublet		64.9	71.5			
cyc doublet	−567.160084	−570.837699	−570.582559	−569.173847	0.033	
lin quartet		82.6	88.7			
cyc quartet	68.3	55.0	54.8	65.2	0.029	
C_{16}^+						
cyc doublet		−608.913566	−608.643390			
cyc quartet		8.7	10.9			
C_{17}^+						
cyc doublet		−646.998694	−646.709065			
cyc quartet		4.7	3.9			
C_{18}^+						
cyc doublet		−685.115588	−684.809946			
cyc quartet		34.2	33.5			
C_{19}^+						
cyc doublet		−723.203832	−722.881376			

[a] Davidson quadruple corrected CI−SD. [b] von Helden, G; Gotts, N. G.; Palke, W. E.; Bowers, M. T. *Int. J. Mass Spectrom. Ion Processes* **1994**, *138*, 33.

TABLE 10. Comparison of the Relative Energies, $\Delta E = E_{\rm lin} - E_{\rm cyc}$ (kcal/mol) of Carbon Clusters at Different Theoretical Levels with Some Experimental Data

species	exptl[a]	ROHF[a]	CI-SD+Q[a,b]	B3LYP	B3PW91	CCSD(T)
C_4^+				−1.2	3.8	2.9
C_5^+				−50.1	−40.9	−46.8
C_6^+				11.2	0.8	−2.9
C_7^+	20 ± 5	8.2	20.5	19.6	24.0	20.9
C_8^+	23 ± 8	5.0	12.0	5.1	13.2	9.1
C_9^+	17 ± 8	20.2	14.4	1.7	8.8	13.1
C_{10}^+	47 ± 8	28.2	40.5	40.7	47.9	46.5
C_{11}^+				49.8	48.5	56.2
C_{12}^+				37.5	43.1	40.6
C_{13}^+				36.8	43.8	47.5
C_{14}^+				64.0	70.5	
C_{15}^+				64.9	71.5	

[a] von Helden, G; Gotts, N. G.; Palke, W. E.; Bowers, M. T. *Int. J. Mass Spectrom. Ion Processes* **1994**, *138*, 33. [b] Davidson quadruple corrected CI-SD.

more recently that the 2053 cm^{-1} feature belongs to the $C_3\cdots H_2O$ complex.

In the IR spectrum of carbon vapor, trapped in an Ar matrix, a number of bands still remain to be assigned: 1346 (weak), 1477 (weak), 1489 (stronger), 1578 (broad), 1747 (weak), 2036 (shoulder of 2041 cm^{-1} (C3(lin))), 2180−2214 (very broad), 2218−2227 (very broad), 2247−2251 (broad) cm^{-1}.

It should be noticed that the computed harmonic frequencies differ from the experimental ones due to the following effects: anharmonicities, interactions of the clusters with the Ar matrix, and spectral shifts due to the matrix. In previous papers,[18] it has been shown that a linear relationship can be established between the ν (observed, matrix) and ω (calculated, B3LYP/cc-pVDZ) frequencies of linear C_n species. If we use such a relationship, it is found that, within the experimental spectrum, the weak band at 1346 cm^{-1} can be due to C_4^+ (doublet, linear) and the bands at 1489 and 1578 cm^{-1} to C_{13}^+ (linear, doublet, quartet). For the line at 2036 cm^{-1}, there are many candidates: C_8^+, C_{10}^+, C_{12}^+, C_{14}^+ (all doublets); C_6^+, C_{10}^+, C_{11}^+, C_{12}^+, C_{15}^+ (all quartets); also cyclic C_{11}^+ (doublet, quartet), C_{15}^+ (quartet) (see Table 11). Potential candidates for the 2180−2217 cm^{-1} region are linear C_5^+ (doublet), C_7^+ (doublet), C_8^+ (quartet); cyclic C_{14}^+ (doublet), C_{17}^+ (doublet). For the 2218−2227 cm^{-1} region, linear C_8^+ (quartet) is the candidate. No linear C_n^+ species studied in the present paper appear to absorb in the 2247−2253 cm^{-1} region.

Clearly, considering the complexity of the IR spectrum in certain regions and the fact that many species absorb in those regions, no definitive assignments of bands can be made. However, the results of our vibrational analysis may help the interpretation of future experimental data.

6. Adiabatic Ionization Potentials. As a direct byproduct of the present study, we provide in Table 12 the adiabatic ionization potential (AIP) of the carbon clusters considered in this study, which have been evaluated from the energies obtained from the B3LYP/cc-pVDZ and CCSD(T)/cc-pVDZ calculations. The B3LYP values have been furthermore corrected for zero-point vibrational energies (to be found in Table 11). As can be seen from this table, the latter have a rather marginal effect on the ionization energies, in general smaller than 0.1 eV. In sharp contrast with the isomerization energies, our B3LYP and CCSD(T) calculations provide very similar values of ionization energies. These are found furthermore to sustain a very satisfactory comparison with previous theoretical results obtained for C_4, C_5, and C_6.[17] Comparison with experiment,[57−59] on the other hand, is only successful with one value reported as *adiabatic* for C_6,[59] leaving us with the idea that the ionization potentials measured[57,58] for C_4 and C_5, being *too small* by 1.6−2.0 eV on the theoretical side [CCSD(T)], are essentially *vertical* in nature.

Either for the linear or cyclic clusters, the adiabatic ionization energies appear globally to decrease with increasing system size (Figure 6), a fact which naturally relates to the construction[42] of the band structure of a stereoregular polymer chain. As for the IR activity, the ionization potentials of linear C_n clusters exhibit a deviation to a regular size dependence with a $2n$ periodicity, whereas the cyclic species present again the characteristic $4n$ periodicity. Quite naturally, in view of the stabilizing resonant effects present in cumulenic species, maxima in the size dependence of the AIP are encountered for rings with a number of carbon atoms equal to $4n + 2$.

From inspection of Figure 6, the C_{4n+2} and to a lesser extent the C_{4n+1} cyclic clusters can be generally characterized by a rather net increase of the AIP, whereas a net reduction is observed with the C_{4n} and C_{4n+3} cyclic species. This ultimate finding beautifully justifies our description of the C_{4n+1} and C_{4n+2} rings, on the one hand, and of the C_{4n} and C_{4n+3} rings on the other hand, as cumulenic and polyynic systems, respectively. Since the influence of the cyclic closure on the electronic and molecular structures will progressively shade off with increasing system size, it is quite clear, however, that this classification should break down for much larger systems.

Quite obviously from Figure 6, the size dependence of the AIP of the largest clusters considered in this study is still far from converging to some asymptotic value, as should be normally expected for a size-intensive property.[60] For very large (i.e., infinite) C_n clusters, the AIP's of rings and chains should furthermore converge to the same limit, which, regardless of dynamic electronic relaxation and correlation effects, should be close to 0 eV, in view of the cumulenic character of the largest linear chains considered here.

Nonetheless and as in many instances,[61] strong failures of Koopmans' theorem[62] must certainly occur,[63] in particular when dealing with the cyclic polyynic species (see, e.g., Figure 2 and section 2). These most often take the form of a reversal of the outermost ionization energies compared to the HF ordering. For instance, for the cyclic C_8 cluster, the ionized $6b_g^{-1}$ state is more stable than the $2b_u^{-1}$ state. This relates[61] to the presence of a low-lying virtual orbital of π-type (the LUMO of the cyclic C_8 cluster has, e.g., a $3b_u$ label) and to many-body effects (in particular, pair relaxation,[64] i.e., the increase of electron correlation due to relaxation and electron excitations into an extra unoccupied orbital). At this stage, it must thus be stressed that the ionization spectra of large carbon clusters still remain a very challenging question, considering also the major breakdown of the orbital picture of ionization[63,65] that can be expected for so strongly correlated compounds.

Conclusions

In the present study, structural and vibrational properties of large cyclic and linear carbon clusters C_n^+ ($n = 4-19$) have been investigated in detail using density functional theory (DFT) and coupled cluster (CC) calculations. Two functionals, i.e., B3LYP (Becke three-parameter Lee−Yang−Parr) and B3PW91 (Becke three-parameter Perdew−Wang), have been considered in conjunction with a correlation-consistent polarized double-ζ (cc-pVDZ) basis in the DFT calculations. The geometries and frequencies obtained with both schemes are virtually the same and compare rather nicely with the results of coupled cluster calculations in the CCSD(T) approximation. Isomerization energies, on the other hand, may show some substantial

TABLE 11. Harmonic Frequencies (cm^{-1}) and IR Intensities (km/mol) of C_n^+ Cations at the B3LYP/cc-pVDZ Level[a]

C$_4^+$	
D_{2h} cyclic doublet ZPE = 6.21	**198(b$_{1u}$,797)**, 339(b$_{3u}$,12), 620(b$_{2u}$,64)
D$_{2h}$ cyclic quartet ZPE = 8.62	574(b$_3$u, 1), 846(b$_{2u}$, 24), **1394(b$_{1u}$, 46)**
D$_{\infty h}$ linear doublet ZPE = 6.19	129(π_u, 12), 149(π_u, 6), **1330(σ_u, 632)**
D$_{\infty h}$ linear quartet ZPE = 7.53	**1914(σ_u, 5495)**
C$_5^+$	
C_s cyclic doublet ZPE = 9.52	325(a′, 343), 349(a″, 1), 582(a′, 1), 606(a′, 2), 831(a′, 12), 1254(a′, 3), **1446(a′, 482)**, 1670(a′, 19)
C$_{2v}$ cyclic quartet ZPE = 12.12	**303(b$_2$, 140)**, 396(b$_2$, 29), 1673(a$_1$, 24)
C$_{\infty v}$ linear doublet ZPE = 10.44	270(π, 2), 595(π, 2), 793(σ, 23), 1466(σ, 152), 2110(σ, 3), **2249(σ, 1802)**
D$_{\infty h}$ linear quartet ZPE = 12.30	153(?, 4), 158(?, 5), 615(?, 6), 1604(σ_u, 7), **1964(σ_u, 881)**
C$_6^+$	
C_{2v} cyclic doublet ZPE = 14.80	364(b$_1$, 3), 476(b$_1$, 1), 563(a$_1$, 29), 1236(a$_1$, 2), 1561(b$_2$, 35), 1778(a$_1$, 50), **2076(b$_2$, 600)**
C$_{2v}$ cyclic quartet ZPE = 14.98	**398(b$_2$, 36)**, 416(a$_1$, 32), 948(b$_2$, 29), 955(a$_1$, 27), 1655(a$_1$, 3), 1657(b$_2$, 3)
D$_{\infty h}$ linear doublet ZPE = 17.61	91(? 6), 99(?, 4), 362(?, 3), 397(?, 1), 1171(σ_u, 448), **2068(σ_u, 1225)**
C$_{\infty v}$ linear quartet ZPE = 14.74	97(π, 1), 211(π, 8), 426(π, 1), 673(σ, 12), 1243(σ, 138), 1769(σ, 127), 1975(σ, 305), **2131(σ, 384)**
C$_7^+$	
C_s cyclic doublet ZPE = 16.63	368(a″, 15), 463(a′, 31), 557(a′, 17), 1241(a′, 8), 1242(a′, 10), 1527(a′, 14), 1618(a′, 32), **1760(a′, 145)**, 1775(a′, 138)
C$_{2v}$ cyclic quartet ZPE = 18.48	139(b$_1$, 3), 391(b$_2$, 27), 432(b$_{1,}$ 1), 960(a$_1$, 4), **1141(b$_2$, 72)**, 1244(b$_2$, 4), 1365(b$_2$, 1), 1717(a$_1$, 2), 1973(a$_1$, 8)
C$_{\infty v}$ linear doublet ZPE = 19.39	178(π, 3), 286(π, 1), 584(σ, 13), 669(π, 3), 1109(σ, 34), 1578(σ, 152), 2083(σ, 919), 2182(σ, 835), **2244(σ, 2189)**
D$_{\infty h}$ linear quartet ZPE = 18.92	83(?, 2), 87(?, 3), 536(?, 1), 673(?, 5), 1129(σ_u, 2), **1889(σ_u, 1884)**, 2075(σ_u, 38)
C$_8^+$	
C_s cyclic doublet ZPE = 20.74	401(a″, 37), 529(a′, 49), 529(a′, 49), 1131(a′, 18), 1803(a′, 389), **1803(a′, 396)**, 1803(a′, 32)
C$_{2v}$ cyclic quartet ZPE = 25.26	348(b$_1$, 2), **509(b$_2$,19)**, **509(a$_1$,19)**, 1523(a$_1$, 18), 1523(b$_2$, 18)
D$_{\infty h}$ linear doublet ZPE = 22.79	61(?, 3), 64(?, 2), 223(?, 8), 241(?, 5), 962(σ_u, 181), 1649(σ_u, 746), **2171(σ_u, 2420)**
D$_{\infty h}$ linear quartet ZPE = 21.55	388(π_g, 14), 1009(σ_u, 112), 1361(π_u, 4942), 1894(σ_u, 1342), **2337(σ_u, 12833)**
C$_9^+$	
C_{2v} cyclic doublet ZPE = 23.26	34(b$_2$, 93), 124(b$_2$, 7), 405(b$_1$, 1), 562(a$_1$, 62), 957(b$_2$, 221), 1136(b$_2$, 79), 1345(a$_1$, 10), 1800(b$_2$, 67), **1955(a$_1$, 341)**, 2001(b$_2$, 163), 2072(a$_1$, 82)
C$_{2v}$ cyclic quartet ZPE = 23.14	157(a$_1$, 1), 284(b$_2$, 3), **351(a$_1$, 19)**, 369(b$_1$, 4), 443(b$_2$, 3), 1058(b$_2$, 1), 1171(b$_2$, 6), 1370(a$_1$, 4), 1536(b$_2$, 1), 1743(a$_1$, 6), 1789(b$_2$, 15), 2037(a$_1$, 2)
C$_{\infty v}$ linear doublet ZPE = 24.24	44(?, 6), 50(?, 2), 125(?, 20), 207(?, 4), 433(?, 4), 716(?, 10), 876(σ, 79), 1575(σ, 362), **1833(σ, 4191)**, 2108(σ, 2122)
D$_{\infty h}$ linear quartet ZPE = 24.23	39(?, 10), 49(?, 2), 104(?, 21), 191(?, 9), 383(?, 7), 421(?, 5), 672(?, 11), 738(?, 1), 849(σ_u, 138), 1483(σ_u, 802), 1826(σ_u, 990), **2019(σ_u, 1357)**
C$_{10}^+$	
C_{2v} cyclic doublet ZPE = 26.42	129(b$_2$, 43), 243(b$_2$, 26), 316(a$_1$, 17), 374(b$_1$, 6), 399(a$_1$, 2), 473(b$_2$, 2), 516(a$_1$, 15), 821(a$_1$, 1), 1053(b$_2$, 1), 1072(a$_1$, 2), 1460(b$_2$, 2), **1521(b$_2$, 100)**, 1585(b$_2$, 9), 1908(a$_1$, 49), 1935(b$_2$, 41), 2096(a$_1$, 92)
C$_{2v}$ cyclic quartet ZPE = 28.11	189(b$_2$, 4), 236(b$_1$, 5), 520(a$_1$, 6), 1009(b$_2$, 8), 1015(b$_2$, 8), 1410(b$_2$, 1), 1512(a$_1$, 1), 1680(a$_1$, 24), 1759(b$_2$, 59), 1798(b$_2$, 13), **1813(b$_1$, 3983)**, 2087(a$_1$, 33)
D$_{\infty h}$ linear doublet ZPE = 28.43	41(? 2), 42(?, 2), 170(?, 8), 183(?, 6), 366(?, 2), 392(?, 1),615(?, 1), 671(?, 2), 800(σ_u, 76), 1471(σ_g,613), 2042(σ_u, 1922), **2199(σ_u, 3170)**
C$_{\infty v}$ linear quartet ZPE = 28.33	108(?, 4), 190(?, 1), 281(?, 2), 416(σ, 5), 808(σ, 11), 1196(σ, 72), 1503(σ, 192), 1836(σ, 269), 1855(σ, 271), 2051(σ, 577), 2123(σ, 161), **2177(σ, 1826)**

TABLE 11 (Continued)

C_{11}^+	
C_{2v} cyclic doublet ZPE = 28.24	65(b_2, 2), 256(a_1, 8), 383(b_1, 13), 394(b_2, 8), 402(b_1, 18), 429(a_1, 20), 466(b_2, 38), 505(a_1, 25), 974(a_1, 6), 989(b_2, 6), 1408(b_2, 1), 1614(b_2, 7), 1710(b_2, 4), 1890(a_1, 22), 1924(a_1, 3), **2025(b_2, 111)**, 2057(a_1, 98)
C_{2v} cyclic quartet ZPE = 30.19	211(a_1, 14), 232(b_2, 1), 323(b_2, 3), 399(b_2, 5), 455(a_1, 33), 504(b_1, 3), 558(a_1, 10), 765(a_1, 2), 832(b_2, 44), 1085(b_2, 6), 1269(a_1, 19), 1377(b_2, 94), 1459(b_2, 31), 1626(b_2, 61), 1864(a_1, 25), **1997(a_1, 350)**, 2100(a_1, 44)
$D_{\infty h}$ linear doublet ZPE = 31.87	34(?, 2), 35(?, 1), 136(?, 13), 157(?, 5), 293(?, 5), 298(?, 1), 736(?, 30), 761(?, 10), 1371(σ_u, 223), **1721(σ_u, 5984)**, 1873(σ_u, 1539), 2181(σ_u, 3022)
$D_{\infty h}$ linear quartet ZPE = 31.07	34(?, 2), 34(?, 1), 135(?, 14), 154(?, 8), 293(?, 6), 350(?, 6), 724(?, 57), 732(?, 8), 1330(σ_u, 661), 1736(σ_u, 2043), 1825(σ_g, 1004), **2099(σ_u, 2115)**
C_{12}^+	
D_{6h} cyclic doublet ZPE = 34.62	511(e_{1u}, 31), 906(e_{1u}, 2), **1741(e_{1u}, 95)**
D_{6h} cyclic quartet ZPE = 34.65	508(e_{1u}, 35), 916(e_{1u}, 4), **1611(e_{1u}, 66)**
$D_{\infty h}$ linear doublet ZPE = 35.22	29(?, 1), 30(?, 1), 134(?, 7), 141(?, 5), 273(?, 4), 282(?, 3), 664(?, 1), 680(σ_u, 33), 716(?, 3), 1278(σ_u, 294), 1722(σ_u, 888), **2128(σ_u, 5552)**, 2191(σ_u, 2268)
$C_{\infty v}$ linear quartet ZPE = 35.08	79(π, 2), 144(π, 1), 217(π, 3), 295(π, 1), 349(σ, 4), 682(σ, 2), 997(σ, 214), 1291(σ, 526), 1567(σ, 43), 1771(σ, 79), 1854(σ, 195), 2037(σ, 10), **2091(σ, 2683)**, 2146(σ, 13), 2194(σ, 1575)
C_{13}^+	
C_1 cyclic doublet ZPE = 36.46	108(?, 1), 469(?, 1), 477(?, 1), 481(?, 1), 503(?, 68), 529(?, 1), 679(?, 24), 811(?, 173), 845(?, 7), **1005(?, 480)**, 1238(?, 7), 1239(?, 6), 1823(?, 1), 2029(?, 108), 2057(?, 258), 2067(?, 367), 2118(?, 366), 2128(?, 124)
C_{2v} cyclic quartet ZPE = 36.99	14(b_2, 4), 396(a_1, 3), 408(b_2, 1), **436(a_1, 7)**, **454(b_2, 7)**, 477(a_1, 2), 504(b_1, 3), 841(b_2, 2), 842(a_1, 1), **1026(b_2, 7)**, 1890(a_1, 3), 1911(b_2, 3)
$D_{\infty h}$ linear doublet ZPE = 37.61	25(?, 1), 25(?, 1), 115(?, 8), 121(?, 4), 234(?, 8), 249(?, 3), 431(?, 1), 614(?, 1), 632(σ_u, 11), 807(?, 10), 1198(σ_u, 106), **1611(σ_u, 7577)**, 1678(σ_u, 2427), 2062(σ_u, 2071), 2205(σ_u, 4029)
$D_{\infty h}$ linear quartet ZPE = 37.78	25(?, 1), 25(?, 1), 116(?, 8), 121(?, 6), 235(?, 8), 241(?, 5), 397(?, 3), 431(?, 1), 626(σ_u, 23), 788(?, 7), 1177(σ_u, 384), **1622(σ_u, 2487)**, 1645(σ_u, 1972), 2021(σ_u, 2187), 2131(σ_u, 2479)
C_{14}^+	
C_{2v} cyclic doublet ZPE = 37.36	147(a_1, 33), 476(a_1, 2), 803(b_2, 3), 819(a_1, 6), 1346(b_2, 91), **2122(a_1, 101)**, 2123(b_2, 78),
C_{2v} cyclic quartet ZPE = 40.57	457(a_1, 1), 791(b_2, 1), 792(b_1, 1), 794(a_1, 2), 1639(a_1, 1), **1653(b_2, 89)**, 1930(b_2,5), 1932(a_1, 55)
$D_{\infty h}$ linear doublet ZPE = 40.97	21(π, 1), 22(π, 1), 105(?, 5), 109(?, 4), 222(?, 6), 231(?, 4), 367(?, 1), 387(?, 1), 589(σ_u, 14), 709(?, 2), 754(?, 4), 1125(σ_u, 145), 1595(σ_u, 853), 2017(σ_u, 2636), **2141(σ_u, 9003)**, 2207(σ_u, 509)
$D_{\infty h}$ linear quartet ZPE = 41.85	21(?, 1), 22(?, 1), 91(?, 16), 108(?, 4), 181(?, 15), 230(?, 5), 364(?, 6), 379(?, 1), 537(?, 2), 582(σ_u, 6), 717(?, 2), 731(?, 3), 1108(σ_u, 201), 1540(σ_u, 475), **1807(σ_u, 3649)**, 1911(σ_u, 2903), 2148(σ_u, 2752)
C_{15}^+	
C_{2v} cyclic doublet ZPE = 42.88	134(b_2, 4), 470(a_1, 2), 486(a_1, 3), 516(a_1, 1), **521(b_1, 21)**, 580(b_2, 7), 757(a_1, 3), 767(b_2, 2), 1831(a_1, 5), 2101(b_2, 3), 2104(a_1, 2), 2127(b_2, 2), 2129(a_1, 2)
C_{2v} cyclic quartet ZPE = 43.74	275(a_1, 5), 321(b_2, 21), 419(b_1, 10), 748(a_1, 2), 752(b_2, 3), 755(b_1, 5), 1164(b_2, 4), 1851(a_1, 1), 1854(b_2, 1), 1912(b_2, 42), 1914(a_1, 42), **2027(b_2, 66)**, 2028(a_1, 64)
$D_{\infty h}$ linear doublet ZPE = 43.94	19(π_u, 1), 19(π_u, 1), 93(?, 6), 95(?, 3), 195(?, 8), 206(?, 4), 256(?, 8), 312(?, 1), 326(?, 3), 553(σ_u, 2), 656(?, 2), 1060(σ_u, 43), 1499(σ_u, 4920), **1527(σ_u, 8547)**, 1891(σ_u, 1493), 2143(σ_u, 3173), 2201(σ_u, 5029)
$D_{\infty h}$ linear quartet ZPE = 44.49	19(π, 1), 19(π, 1), 93(?, 5), 96(?, 4), 197(?, 8), 204(?, 6), 327(?, 3), 364(?, 3), 549(σ_u, 7), 839(?, 6), 1049(σ_u, 220), 1489(σ_u, 1518), 1548(σ_g, 4943), 1851(σ_u, 1214), **2095(σ_u, 5289)**, 2136(σ_u, 1259)
C_{16}^+	
D_{8h} cyclic doublet ZPE = 45.64	499(?, 30), 717(?, 8), **1693(?, 247)**
D_{8h} cyclic quartet ZPE = 47.13	499(?, 35), 722(?, 11), **1482(?, 181)**
C_{17}^+	
C_{2v} cyclic doublet ZPE = 50.55	21(b_2, 10), 82(b_2, 8), 445(a_1, 37), 499(b_2, 4), 523(b_1, 1), 525(b_2, 2), 573(a_1, 60), 579(b_1, 1), 647(b_2, 303), 676(a_1, 15), 811(b_2, 876), 1016(?, 6), 1016(?, 4), 2073(b_2, 6), **2100(a_1, 908)**, 2108(b_2, 630), 2123(a_1, 257), 2177(b_2, 70), 2177(a_1, 65)
C_{2v} cyclic quartet ZPE = 49.70	451(a_1, 5), 455(b_2, 4), 483(b_2, 3), 486(a_1, 4), 648(b_1, 2), 672(a_1, 4), 673(b_2, 4), 866(b_2, 5), 1839(a_1, 5), **1892(b_2, 7)**, 1926(a_1, 2)
C_{18}^+	
C_{2v} cyclic doublet ZPE = 54.16	277(b_2, 25), 498(b_2, 3), 640(a_1, 8), 656(b_2, 10), **1102(a_1, 195)**, 2158(b_2, 145), 2160(a_1, 112)
C_{2v} cyclic quartet ZPE = 51.90	118(b_2, 2), 481(a_1, 1), 556(b_1, 18), 620(a_1, 4), 637(b_2, 3), 1305(a_1, 3), 1309(b_2, 1), **1639(a_1, 484)**, 2003(b_2, 96), 2050(b_2, 122), 2074(a_1, 58)
C_{19}^+	
C_{2v} cyclic doublet ZPE = 57.45	479(b_2, 8), 514(b_2, 3), 556(a_1, 2), 565(b_2, 18), 616(a_1, 7), 688(b_1, 4), 728(b_1, 8), **1716(a_1, 32)**, 2073(b_2, 8), 2077(a_1, 5)

[a] Only IR active modes with intensity ≥1 km/mol are given. The most stable isomer is displayed in bold as well as the most intense harmonic frequencies. The zero-point energies (ZPE) are expressed in kcal/mol. (?) indicates that no definite symmetry assignment of the harmonic vibration modes was possible from the GAUSSIAN94 outputs.

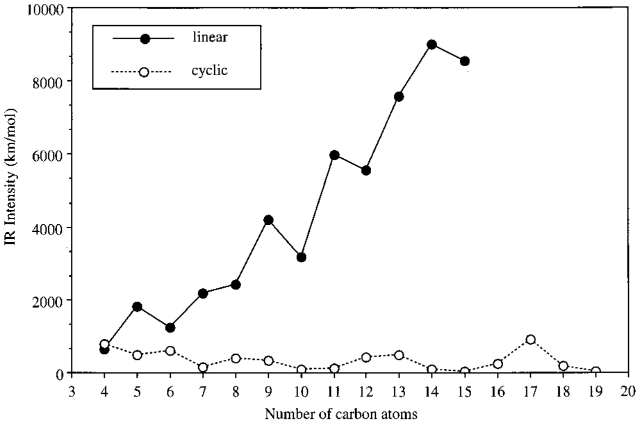

Figure 4. The IR activity associated with the most intense line of linear and cyclic carbon clusters.

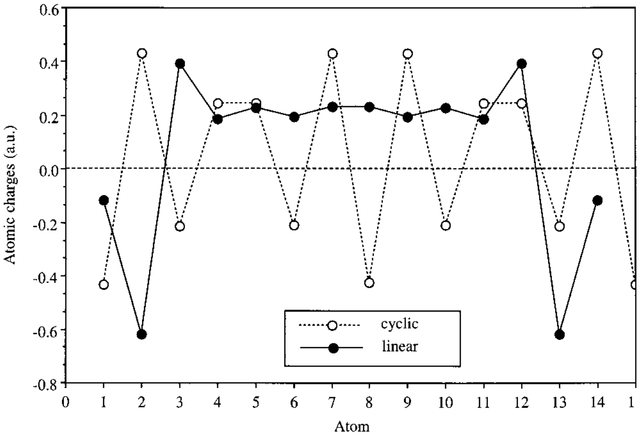

Figure 5. Distribution of electric charges within the linear and cyclic forms of the C_{14}^+ cluster (results of a Mulliken population analysis of a HF/cc-pVDZ calculation).

deviations. Calculated isomerization energies compare fairly well with a few available experimental data available for C_n^+ ($n = 7-10$) species, indicating that DFT and CCSD(T) can be used as reliable tools to investigate the structure and energetics of highly correlated systems such as carbon cluster cations.

Compared to the results of ROHF calculations, electronic correlation effects strongly limit distortions toward strongly alternating structures, as could be expected from severe electronic degeneracies in the wave functions of, e.g., cyclic C_6^+ or C_{10}^+. Despite the importance of electron correlation, carbon clusters exhibit upon adiabatic ionization behaviors that are reminiscent of very simple topological rules drawn from the tight-binding or Hückel picture, in particular in regards to the aromaticity or antiaromaticity of rings containing $4n + 2$ and $4n$ vertices, respectively. As for the neutral species, the cyclic C_{4n+2}^+ clusters present a regular, i.e., cumulenic, structure, whereas cyclic carbon clusters C_{4n}^+ are clearly alternating, i.e., polyynic. From the variations in bond length alternations, it has been found that the cumulenic C_{4n+2} rings tend to become more polyynic upon adiabatic ionization, whereas the opposite trend is observed for the polyynic C_{4n} rings. This is true also, to a lesser extent, for the C_{4n+1} and C_{4n+3} cyclic clusters, which according to their behavior under ionization, can be regarded as dominantly cumulenic or polyynic, respectively. On the other hand, the linear clusters only evolve from an essentially cumulenic structure in their neutral forms to a structure with a more pronounced polyynic character after ionization. In this case, the amplitude of these distortions decreases rather rapidly with the size of chains.

TABLE 12. Adiabatic Ionization Potentials (eV) of Carbon Clusters, Obtained Using the B3LYP and the CCSD(T) Approaches[a,b]

		B3LYP/cc-pVDZ		CCSD(T)/cc-pVDZ	
		doublet	quartet	doublet	quartet
C_4	cyclic	10.6 (−0.070)	11.2 (+0.028)	10.3	11.0
	linear	11.1 (−0.039)	11.5 (+0.008)	9.4	9.6
C_5	cyclic	10.1 (+0.012)	11.0 (−0.028)	10.0	10.9
	linear	11.0 (−0.012)	12.3 (−0.020)	10.5	12.0
C_6	cyclic	10.3 (+0.019)	11.1 (−0.103)	9.9	10.9
	linear	10.0 (−0.027)	10.3 (−0.017)	8.2	8.7
C_7	cyclic	8.3 (+0.035)	11.1 (−0.084)	8.2	11.0
	linear	10.2 (−0.015)	11.5 (−0.034)	9.7	11.1
C_8	cyclic	8.4 (−0.013)	9.0 (−0.101)	8.5	9.1
	linear	9.3 (−0.020)	10.4 (+0.141)	7.6	8.9
C_9	cyclic	8.6 (−0.002)	8.9 (−0.045)	8.2	8.7
	linear	9.3 (−0.074)	10.5 (−0.121)	9.1	10.6
C_{10}	cyclic	9.1 (−0.080)	12.5 (−0.167)	9.0	12.7
	linear	8.4 (−0.018)	9.0 (−0.028)	8.2	11.2
C_{11}	cyclic	7.5 (+0.002)	9.7 (−0.130)	7.6	9.7
	linear	8.8 (−0.067)	9.8 (−0.105)	8.6	9.9
C_{12}	cyclic	7.8 (−0.039)	8.2 (−0.065)	8.2	8.5
	linear	8.0 (−0.014)	8.7 (−0.033)	7.9	11.4
C_{13}	cyclic	7.7 (−0.005)	7.9 (−0.055)		
	linear	8.4 (−0.066)	9.3 (−0.100)		
C_{14}	cyclic	8.3 (−0.066)	10.8 (−0.223)		
C_{15}	cyclic	7.1 (−0.016)	9.4 (−0.062)		
C_{16}	cyclic	7.3 (−0.155)	7.7 (−0.090)		
C_{17}	cyclic	7.3 (−0.0005)	7.5 (−0.038)		
C_{18}	cyclic	7.8 (−0.042)	9.2 (−0.140)		
C_{19}	cyclic	6.4 (+0.036)			

[a] B3LYP results incorporate the variations of zero-point vibrational energies (in parentheses). [b] Available experimental values: aIP(C_4), 12.6 eV;[57] aIP(C_5), 12.5 ± 0.1 eV,[57] 12.7 ± 0.5 eV;[58] aIP(C_6), 12.54 ± 0.3 eV,[58] 9.6 ± 0.3 eV.[59]

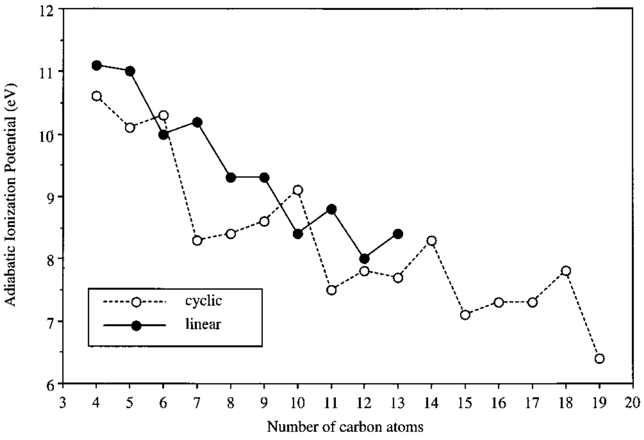

Figure 6. Size dependence of the adiabatic ionization potential of linear and cyclic C_n clusters.

The linear carbon cations exhibit a much more pronounced IR intensity than the cyclic ones. Many of the studied species show a strong absorption in certain regions of the spectrum (e.g., around 2036 cm^{-1}). No linear C_n^+ species ($n = 4-15$) appear to absorb in the 2247−2253 cm^{-1} region where IR activity has been observed experimentally.

A main conclusion of the present study is that detailed investigations of the adiabatic ionization process of carbon clusters can provide very specific insights into their electronic and structural properties. Specific markers of the cumulenic or polyynic character of carbon chains or rings that could possibly be exploited in future experimental investigations are provided by the adiabatic ionization potentials and the contrasted structural modifications induced by ionization, which can be indirectly traced from the symmetry of the inertia tensor and the infrared activity.

Acknowledgment. M.S.D. thanks the "Fonds voor Wetenschappelijk Onderzoek van Vlaanderen", the Flemish Science Foundation, for his senior research assistant position at the Limburgs Universitair Centrum. M.G.G. acknowledges financial support from the "Bijzonder Onderzoeksfonds" (BOF) of the Limburgs Universitair Centrum. The authors warmly acknowledge computational support from Prof. J. Martin, Department of Organic Chemistry, Weizmann Institute of Science, Rehovot, Israel, where some of the calculations presented here have been performed (namely, the CCSD(T) calculations for the $C_{12}^+-C_{15}^+$ clusters in their cyclic form). The authors also thank Dr. J. El-Yazal for his kind help.

Supporting Information Available: Atomic cartesian coordinates of the C_n^+ ($n = 4-19$) clusters optimized via DFT/B3LYP calculations in conjunction wiht the cc-pVDZ basis set. This material is available free of charge via the Internet at http://pubs.acs.org.

References and Notes

(1) Weltner, W., Jr.; Van Zee, R. J. *Chem. Rev.* **1989**, *89*, 1713; *J. Mol. Struct.* **1990**, *222*, 201.

(2) Hutter, J.; Lüthi, H. P.; Diederich, F. *J. Am. Chem. Soc.* **1994**, *116*, 750.

(3) Martin, J. M. L.; Taylor, P. R. *J. Phys. Chem.* **1996**, *100*, 6047.

(4) Raghavachari, K.; Curtiss, L. A. Accurate Theoretical Studies of Small Elemental Clusters. In *Quantum Mechanical Electronic Structure Calculations with Chemical Accuracy*; Langhoff, S. R., Ed.; Kluwer: Dordrecht, 1995.

(5) Krätschmer, W.; Nachtigall, K. In *Polycyclic Aromatic Hydrocarbons and Astrophysics*; Lèger, A., et al., Eds.; Reidel: Dordrecht, 1987.

(6) Cermak, I.; Monninger, G.; Krätschmer, W. *Advances in Molecular Structure Research*; JAI Press, 1997; Vol. 3, pp 117−146.

(7) Bollick, E. A.; Ramsey, D. A. *J. Chem. Phys.* **1958**, *29*, 1418; *Astrophys. J.* **1963**, *137*, 84.

(8) Hinkle, K. H.; Keady, J. J.; Bernath, P. F. *Science* **1988**, *241*, 1319 and references therein.

(9) Celii, F. G.; Butler, J. E. *Annu. Rev. Phys. Chem.* **1991**, *42*, 643 and references therein. Levy Guyer, R.; Koshland, D. E., Jr. *Science* **1990**, *250*, 1640.

(10) ZFI Mitteilungen, nr. 134: Beiträge zur Clusterforschung, Academie der Wissenschaften der DDR, September 1987.

(11) Curl, R. F. *Rev. Mod. Phys.* **1997**, *69*, 691.

(12) Kroto, H. *Rev. Mod. Phys.* **1997**, *69*, 703.

(13) Smalley, R. F. *Rev. Mod. Phys.* **1997**, *69*, 723.

(14) Dresselhaus, M. S.; Dresselhaus, G.; Eklund, P. C. *Science of Fullerenes and Carbon Nanotubes*; Academic Press: New York, 1996.

(15) Hare, J. P.; Hsu, W. K.; Kroto, H. W.; Lappas, A.; Prassides, K.; Terrones, M.; Walton, D. R. M. *Chem. Mater.* **1996**, *8*, 6.

(16) Edwards, J. B. *Combustion: Formation and Emission of Trace Species*; Ann Arbor Science: Ann Arbor, MI, 1974.

(17) Raghavachari, K.; Binkley, J. S. *J. Chem. Phys.* **1987**, *87*, 2191.

(18) Martin, J. M. L.; El-Yazal, J.; François, J. P. *Chem. Phys. Lett.* **1995**, *242*, 570; **1996**, *252*, 9.

(19) Brown, W. L.; Freeman, R. R.; Raghavachari, K.; Schlüter, M. *Science* **1987**, *235*, 860.

(20) Radi, P. P.; von Helden, G.; Hsu, M. T.; Kemper, P. R., Bowers, M. T. *Int. J. Mass Spectrom. Ion Processes* **1991**, *109*, 49. von Helden, G.; Hsu, M. T.; Gotts, N. G.; Bowers, M. T. *J. Phys. Chem.* **1993**, *97*, 8182.

(21) Kemper, P. R.; Bowers, M. T. *J. Phys. Chem.* **1991**, *95*, 5134.

(22) von Helden, G.; Gotts, N. G.; Palke, W. E.; Bowers, M. T. *Int. J. Mass Spectrom. Ion Processes* **1994**, *138*, 33. von Helden, G.; Gotts, N. G.; Bowers, M. T. *Chem. Phys. Lett.* **1993**, *212*, 24.

(23) Kroto, H. W.; Walton, D. R. M. *The Fullerenes. New Horizons for the Chemistry, Physics and Astrophysics of Carbon*; Cambridge University Press: New York, 1993.

(24) (a) Peierls, R. E. *Quantum Theory of Solids*; Clarendon Press: Oxford, 1955. (b) Walatka, V. V.; Labes, M. M.; Perlstein, J. H. *Phys. Rev. Lett.* **1973**, *31*, 1139. (c) Greene, L.; Street, G. B.; Suter, L. J. *Phys. Rev. Lett.* **1977**, *38*, 1305.

(25) Harris, D. C.; Bertolucci, M. D. *Symmetry and Spectroscopy*; Dover Publications: New York, 1989.

(26) Vala, M.; Chandrasekhar, T. M.; Szczepanski, J.; Pellow, R. *J. Mol. Struct.* **1990**, *222*, 209.

(27) Parr, R. G.; Wang, W. *Density-Functional Theory of Atoms and Molecules*; Oxford University Press: New York, 1989.

(28) Raghavachari, K.; Trucks, G. W.; Head-Gordon, M.; Pople, J. A. *Chem. Phys. Lett.* **1989**, *157*, 479.

(29) Hample, C.; Peterson, K.; Werner, H. J. *Chem. Phys. Lett.* **1992**, *190*, 1.

(30) Lee, J. T.; Scuseria, E. G. Achieving Chemical Accuracy with Coupled-Cluster Theory. In *Quantum Mechanical Electronic Structure Calculations with Chemical Accuracy*; Langhoff, S. R., Ed.; Kluwer: Dordrecht, 1995.

(31) Andersson, K.; Malmqvist, P-Å.; Roos, B. O.; Sadlej, A. J.; Wolinski, K. *J. Phys. Chem.* **1990**, *94*, 5483.

(32) Martin J. M. L.; El-Yazal, J.; François, J.-P. *Mol. Phys.* **1995**, *86*, 1437.

(33) Becke, A. D. *J. Chem. Phys.* **1993**, *98*, 5648.

(34) Lee, C.; Yang, W.; Parr, R. G. *Phys. Rev.* **1988**, *37B*, 785.

(35) Perdew, J. P. In *Electronic Structure of Solids*; Ziesche, P., Eschrig, H., Eds.; Akademic Verlag: Berlin, 1991. Perdew, J. P. *Physica* **1991**, *B172*, 1.

(36) Dunning, T. H., Jr. *J. Chem. Phys.* **1989**, *90*, 1007.

(37) Frisch, M. J.; Trucks, G. W.; Schlegel, H. B.; Gill, P. M. W.; Johnson, B. G.; Robb, M. A.; Cheeseman, J. R.; Keith, T.; Petersson, G. A.; Montgomery, J. A.; Raghavachari, K.; Al-Laham, M. A.; Zakrzewski, V. G.; Ortiz, J. V.; Foresman, J. B.; Cioslowski, J.; Stefanov, B. B.; Nanayakkara, A.; Challacombe, M.; Peng, C. Y.; Ayala, P. Y.; Chen, W.; Wong, M. W.; Andres, J. L.; Replogle, E. S.; Gomperts, R.; Martin, R. L.; Fox, D. J.; Binkley, J. S.; Defrees, D. J.; Baker, J.; Stewart, J. P.; Head-Gordon, M.; Gonzalez, C.; Pople, J. A. *GAUSSIAN 94*, revision B.1; Gaussian, Inc.: Pittsburgh, PA, 1995.

(38) MOLPRO 94 is an ab initio MO package by Werner, H.-J.; Knowles, P. J. with contributions from Almlöf, J.; Amos, R. D.; Deegan, M. J. O.; Elbert, S. T.; Hampel, C.; Meyer, W.; Peterson, K.; Pitzer, R.; Stone, A. J.; Taylor, P. R. (University of Birmingham, 1996).

(39) Stanton, J. F.; Gauss, J.; Watts, J. D.; Lauderdale, W. J.; Bernholdt, D. E.; Bartlett, R. J. *ACES II, an ab initio program system*; Quantum Theory Project, University of Florida: Gainesville, FL, 1992. This package includes: Almlöf, J.; Taylor, P. R. *MOLECULE, a vectorized Gaussian integral program*. Helgaker, T.; Jørgensen, P.; Jensen, H. J. A.; Olsen, J.; Taylor P. R. *ABACUS, a Gaussian integral derivative and molecular properties program*. See also: Stanton, J. F.; Gauss, J.; Watts, J. D.; Lauderdale, W. J.; Bernholdt, D. E.; Bartlett, R. J. *Int. J. Quantum Chem. Symp.* **1992**, *26*, 879.

(40) Giuffreda, M. G. Unpublished results.

(41) March, J. *Advanced Organic Chemistry*; Wiley & Sons: New York, 1985.

(42) André, J.-M.; Delhalle, J.; Brédas, J.-L. *Quantum Chemistry Aided of Organic Polymers*; World Scientific Lecture and Course Notes in Chemistry 2; World Scientific Publishing: River Edge, NJ, 1991.

(43) Jahn, H. A.; Teller, E. *Proc. R. Soc.* **1937**, *A161*, 220.

(44) Vosko, S. H.; Wilk, L.; Nusair, M. *Can. J. Phys.* **1980**, *58*, 1200.

(45) Becke, A. D. *J. Chem. Phys.* **1988**, *88*, 2547.

(46) Perdew, J. P. *Phys. Rev. B* **1986**, *33*, 8822.

(47) Godbout, N.; Salahub, D. R.; Andzelm, J. W.; Wimmer, E. *Can. J. Chem.* **1992**, *70*, 560.

(48) Herzberg, G. *Molecular Spectra and Molecular Structure. Infrared and Raman spectra of polyatomic molecules*; van Nostrand Reinhold: New York, 1945. Kroto, H. W. *Molecular Rotation Spectra*; Dover Publications: New York, 1992.

(49) Zare, R. N. *Angular Momentum*; J. Wiley: New York, 1988.

(50) Kemper, P. R.; Bowers, M. T. *J. Am. Chem. Soc.* **1990**, *112*, 3231.

(51) Lee, T. J.; Taylor, P. R. *Int. J. Quantum Chem. Symp*. **1989**, *23*, 199.

(52) Martin, J. M. L.; Lee, T. J.; Scuseria, G. E.; Taylor, P. R. *J. Chem. Phys.* **1997**, *9*, 6549.

(53) (a) André, J.-M. In *Large Finite Systems*; Jortner, J., et al., Eds.; D Reidel: Dordrecht; 1997; p 277. (b) Deleuze, M.; Delhalle, J.; Pickup, B. T. *Theor. Chim. Acta* **1992**, *82*, 309.

(54) Szczepanski, J.; Ekern, S.; Chapo, C.; Vala, M. *Chem. Phys.* **1996**, *211*, 359.

(55) Szczepanski, J.; Ekern, S.; Vala, M. *J. Phys. Chem. A* **1997**, *101*, 1941.

(56) Szczepanski, J.; Ekern, S.; Vala, M. *J. Phys. Chem.* **1995**, *99*, 8002.

(57) Drowart, J.; Burns, R. P.; Demaria, G.; Inghram, M. G. *J. Chem. Phys.* **1959**, *31*, 1131.

(58) Dideler, V. H.; Reese, R. M.; Franklin, J. L. *J. Am. Chem. Soc.* **1961**, *93*, 1813.

(59) Bach, S. B. H.; Eyler, J. R. *J. Chem. Phys.* **1990**, *92*, 358.

(60) (a) Deleuze, M.; Delhalle, J.; Pickup, B. T.; Calais, J.-L. *Phys. Rev. B* **1992**, *46*, 15668. (b) Deleuze, M.; Delhalle, J.; Pickup, B. T.; Calais,

J.-L. *Adv. Quantum Chem.* **1995**, *26*, 35. (c) Deleuze, M.; Scheller, M. K.; Cederbaum, L. S. *J. Chem. Phys.* **1995**, *103*, 3578. (d) Deleuze, M.; Cederbaum, L. S. *Phys. Rev. B* **1996**, *53*, 13326. (e) Deleuze, M.; Cederbaum, L. S. *J. Chem. Phys.* **1996**, *105*, 7583. (f) Deleuze, M.; Cederbaum, L. S. *Adv. Quantum Chem.*, in press.

(61) (a) Cederbaum, L. S.; von Niessen, W. *Chem. Phys. Lett.* **1974**, *24*, 263. (b) Cederbaum, L. S. *Chem. Phys. Lett.* **1974**, *25*, 562. (c) Cederbaum, L. S.; Domcke, W.; Schirmer, J.; von Niessen, W. *Phys. Scrip.* **1980**, *21*, 481.

(62) Koopmans, T. *Phys. (Utr.)* **1933**, *1*, 104.

(63) Ortiz, J. V.; Zakrzewski, V. G. *J. Chem. Phys.* **1994**, *100*, 6614.

(64) Szabo, A.; Ostlund, N. S. *Modern Quantum Chemistry;* Macmillan: New York, 1982.

(65) (a) Deleuze, M. S.; Giuffreda, M. G.; François, J.-P.; Cederbaum, L. S. Valence one-electron and shake-up ionization bands of carbon clusters. I. The C_n ($n = 3, 5, 7, 9$) chains. Submitted. (b) Deleuze, M. S.; Giuffreda, M. G.; François, J.-P.; Cederbaum, L. S. Valence one-electron and shake-up ionization bands of carbon clusters. II. The C_n ($n = 4-10$) rings. To be submitted.